On the Road to 5G: Comparative Study of Physical Layer in MTC Context

Yahia Medjahdi, Sylvain Traverso, Robin Gerzaguet, Hmaied Shaiek, Rafik Zayani, David Demmer, Rostom Zakaria, Jean-Baptiste Doré, Mouna Ben Mabrouk, Didier Le Ruyet, et al.

IEEE Access
Multidisciplinary | Rapid Review | Open Access Journal

Received September 14, 2017, accepted October 14, 2017, date of publication November 15, 2017,
date of current version December 22, 2017.

Digital Object Identifier 10.1109/ACCESS.2017.2774002

On the Road to 5G: Comparative Study of Physical Layer in MTC Context

YAHIA MEDJAHDI[1,2], SYLVAIN TRAVERSO[3], ROBIN GERZAGUET[4], HMAIED SHAÏEK[1], RAFIK ZAYANI[5], DAVID DEMMER[4], ROSTOM ZAKARIA[1], JEAN-BAPTISTE DORÉ[4], MOUNA BEN MABROUK[6], DIDIER LE RUYET[1], (Senior Member, IEEE), YVES LOUËT[6], AND DANIEL ROVIRAS[1], (Senior Member, IEEE)

[1]Conservatoire National des Arts et Métiers, 75003 Paris, France
[2]Institut Supérieur d'Électronique de Paris, 75006 Paris, France
[3]THALES Communications and Security, F-93230 Gennevilliers, France
[4]CEA-Leti, Minatec Campus, 38054 Grenoble, France
[5]Innov'Com, Sup'Com, Carthage University, Ariana 2083, Tunisia
[6]CentraleSupelec, IETR/SUPELEC, 35510 Cesson-Sévigné, France

Corresponding author: Yahia Medjahdi (yahia.medjahdi@isep.fr)

This work was supported by the framework of the WONG5 Project, through the French National Research Agency (ANR) under Grant ANR-15-CE25-0005.

ABSTRACT During the past few years, we are witnessing the emergence of 5G and its high-level performance targets. Waveform (WF) design is one of the important aspects for 5G that received considerable attention from the research community in recent years. To find an alternative to the classical orthogonal frequency division multiplexing (OFDM), several multicarrier approaches addressing different 5G technical challenges, have been proposed. In this paper, we focus on critical machine-type communications (C-MTC), which is one of the key features of the foreseen 5G system. We provide a comparative performance study of the most promising multicarrier WFs. We consider several C-MTC key performance indicators: out-of-band radiations, spectral efficiency, end-to-end physical layer latency, robustness to time and frequency synchronization errors, power fluctuation, and transceiver complexity. The investigated multicarrier WFs are classified into three groups based on their ability to keep the orthogonality: in the complex domain, e.g., most of the OFDM-inspired WFs, in the real domain like offset-quadrature amplitude modulation (QAM)-based techniques, and non-orthogonal WFs like generalized frequency division multiplexing and filter bank-based multicarrier-QAM. Finally, the performances of these WFs are thoroughly discussed in order to highlight their pros and cons and permit a better understanding of their capabilities in the context of C-MTC.

INDEX TERMS Waveforms, 5G, MTC, OFDM, WOLA-OFDM, UF-OFDM, filtered OFDM, N-Cont. OFDM, FMT, FBMC-OQAM, WCP-COQAM, FBMC-QAM, GFDM, BF-OFDM, FFT-FBMC.

I. INTRODUCTION

The fourth generation of wireless network (4G) is currently massively rolled-out but it is also known that it will quickly reach its limits. To face this issue, 3GPPP started to discuss 5G requirement during the RAN 5G workshop held in September 2015 leading to an emerging consensus that there will be a new, non-backward compatible, radio access technology as part of 5G [1], [2].

5G will have to cope with a high degree of heterogeneity in terms of services and requirements. Among these latter, massive Mobile Type Communications (MTC) corresponds to applications that involve a very large number of devices and is recognized as one of the key feature in the upcoming 5G [3]. The vision of 2020 and beyond also includes a significant amount use cases considering a massive number of devices with a wide range of characteristics and demands [4]. It includes low-cost/long-range/low-power MTC as well as broadband MTC with some characteristics more comparable to human-type communication [3].

Besides this, as the availability of large amount of contiguous spectrum is getting more and more difficult to guarantee, the aggregation of non-contiguous frequency bands is considered to meet higher data rates and/or improve access flexibility [2], [5]. This requirement of spectrum agility has encouraged the study for alternative multicarrier waveforms (WFs) to provide better adjacent channel leakage

performance without compromising spectral efficiency. On the other hand, sporadic access has been identified as one of the significant challenges future mobile access networks will have to face [6]. Consequently, relaxed synchronization schemes have been considered to limit the amount of required signaling. In the MTC context, the massive number of devices and the support of multi-point transmissions will imply the use of relaxed synchronization, potentially leading to strong inter-user interference.

Even though Orthogonal Frequency Division Multiplexing (OFDM) is the most prominent multi-carrier modulation technique in wireless standards for below 6GHz transmission, it also exhibits some intrinsic drawbacks. An important frequency leakage is caused by its rectangular pulse shape; the Cyclic Prefix (CP) insertion drives to a spectral efficiency loss; and fine time and frequency synchronization is required to preserve the subcarrier orthogonality that guarantees a low level of intra and inter-cell interferences.

To overcome these limitations, several alternative candidates have been intensively studied in the literature in the past few years. They all apply some kind of filtering and/or windowing operation in either time or frequency domain. For instance, Weighted Overlap and Add OFDM (WOLA-OFDM) [7] or filtered OFDM (f-OFDM) [8] apply the filtering or the windowing operation in time domain. N-Continuous OFDM consists in the use of N derivatives to create a continuous OFDM signal and thus improves the spectral containment [9]. Filter Bank Multicarrier (FBMC) [10]–[13] and Filtered MultiTone (FMT) [14] filter the data in frequency domain at a subcarrier level. Universal Filtered OFDM (UF-OFDM or UFMC) [15] applies the filtering operation in frequency domain, at the Resource Block (RB) level. Same approach is used for Block-Filtered OFDM (BF-OFDM) [16] and Fast Fourier Transform FBMC (FFT-FBMC) [17]. Generalized Frequency Division Multiplexing (GFDM) use a circular convolution to directly apply the filtering operation on a time-frequency block [18]. The different WFs can be classified into different classes, depending on their ability to maintain the orthogonality (or quasi orthogonality) in the real or the complex domain. Some WFs can also be non-orthogonal and manage the self-interference at a sufficiently low level. The additional filtering operation of the post-OFDM WFs allows a better frequency containment and thus enhance performance in coexistence scenarios. However, due to intrinsic difference on how the filtering or the windowing operation is applied, the study, evaluation and comparison of the different WFs is of paramount importance. In this paper we introduce, classify and compare thirteen of the WF candidates: CP-OFDM, WOLA-OFDM, UF-OFDM, f-OFDM, N-continuous OFDM, FMT, FFT-FBMC, BF-OFDM, FBMC-OQAM, Lapped-OFDM, Windowed Cyclic Prefix-based Circular-OQAM (WCP-COQAM), FBMC-QAM and GFDM.

Many studies have already focused on the introduction or the comparison of different WFs candidates. However, they mainly address fewer candidates and/or fewer scenarios than we propose. In [19], OFDM and FBMC (both QAM and OQAM) are compared in terms of achievable SE in different scenarios, channel models and bandwidths. It however does not include the potential benefits of a multi-user access scheme, and the impact of FBMC parametrization. A very detailed analysis on the prototype filter choice for FBMC is done in [20]. Several filters are compared based on different design criteria but direct use-cases for WF evaluation and comparison with classic CP-OFDM are not considered. A direct comparison between OFDM and FBMC has been done in [21]. Different prototype filters are studied, and the analysis of the time frequency behavior of the WFs is done with the use of the ambiguity surface. Again this paper does not provide evaluation results in typical use-case scenarios. In [22], a fair comparison is done between UF-OFDM, OFDM, FBMC and GFDM. However, this paper does not evaluate the complexity and does not neither consider OFDM with filters/windowing (WOLA-OFDM and f-OFDM). In [23], OFDM and DFT-based WFs are compared against several millimeter wave impairments. FBMC based WFs and UF-OFDM are not considered. References [16] and [24]–[28] provide performance comparison in asynchronous multi-user asynchronous scenario but with only a subset of WFs we consider. In [29], the spectral confinement of CP-OFDM, UF-OFDM, fOFDM, GFDM and FBMC-OQAM/QAM is assessed taking into account amplification induced Out-Of-Band (OOB) emissions. We propose in this paper to extend the comparison of the frequency localization to more WFs but without considering non-linearities in order to assess the WF capabilities independently of the radio frequency front-end impairments. Finally an introduction of promising single and multi-carrier WFs has been done in [30]. Detailed evaluation results are nevertheless not included. The main purpose of this paper is to propose a common framework for the evaluation of the different WF candidates in different representative scenarios.

In this paper, we introduce and compare these WFs regarding a given system model and different Key Performance Indicators (KPI). A discussion that puts in perspectives the main advantages and drawbacks of each solution concludes this study. The main contributions of the paper, in addition to be a comprehensive study of some of the most promising multicarrier WFs in expected MTC scenarios, are: i) to propose an unified scenario to evaluate and compare the different WFs. ii) to provide the analysis of some important KPIs providing a fair comparison between the WFs iii) to initiate a discussion that allows a deep understanding of the main challenges MTC physical layer will have to face.

The remainder of the paper is organized as follows. The WF candidates along with their associated transceivers are described in section II. The common comparison framework is described in Section III. Performance and comparison are assessed in Section IV. A fair comparison and a discussion is drawn in section V. Eventually the last section concludes this study.

TABLE 1. WFs key design features.

Orth.	WFs	Filtering			Windowing side	GI
		side	granularity	convolution		
$\mathbb{C}$	CP-OFDM	n/a	n/a	n/a	n/a	CP
	WOLA-OFDM	n/a	n/a	n/a	Tx/Rx	CP
	UF-OFDM	Tx	RB	linear	Rx	ZP
	f-OFDM	Tx/Rx	Sub-band	linear	n/a	CP
	N-Cont.-OFDM	n/a	n/a	n/a	n/a	CP
	FMT	Tx/Rx	subcarrier	linear	n/a	n/a
	FFT-FBMC	Tx/Rx	RB	linear	n/a	CP
	BF-OFDM	Tx	RB	linear	n/a	CP
$\mathbb{R}$	FBMC-OQAM	Tx/Rx	subcarrier	linear	n/a	n/a
	Lapped-OFDM	Tx/Rx	subcarrier	linear	n/a	n/a
	WCP-COQAM	Tx/Rx	subcarrier	circular	Rx	CP
Non Orth.	FBMC-QAM	Tx/Rx	subcarrier	linear	n/a	n/a
	GFDM	Tx/Rx	subcarrier	circular	n/a	CP

II. WAVEFORMS BACKGROUND

A. WAVEFORM CLASSIFICATION

In this paper, the considered multicarrier techniques are classified with respect to the orthogonality which is a key-design property. A given multicarrier WF is orthogonal when it ensures a near perfect recovery of data symbols, very low inter-symbol interference (ISI) and inter-carrier interference (ICI) with a free-distortion channel (perfect and noiseless channel). Based on this definition, we split the different WFs into three categories:

- Orthogonality with respect to the complex domain $\mathbb{C}$: we transmit in this case complex-valued data symbols every symbol period T with a subcarrier spacing F, where the symbol density $TF \geq 1$.
- Orthogonality with respect to the real domain $\mathbb{R}$: Due to the use of time-frequency well-localized prototype function, the orthogonality is restricted to $\mathbb{R}$ by transmitting real-valued data symbols [31]. In order to maintain the symbol density at $TF = 1$, two real-valued symbols are transmitted per unit time-frequency lattice area. In such a case, we find offset-QAM (OQAM)-based WFs.
- Non-orthogonality: Despite the advantages of the previous category, more sophisticated receivers are required when considering OQAM-based WFs in combination with MIMO space-time/frequency block coding (STBC, STBF) techniques due to the high level of inherent interference brought by the prototype filter. In order to overcome this problem, an interesting approach, based on relaxing the orthogonality constraint while transmitting complex-valued data symbols with well-localized time-frequency filters, has been proposed.

Some of the key design features of the considered WFs are summarized in Table 1. More details about these WFs are provided in the following sections.

B. WFs WITH COMPLEX ORTHOGONALITY

1) CP-OFDM (WF01)/WOLA-OFDM (WF02)

In order to maintain the benefits of CP-OFDM while reducing the OOB emissions, straightforward enhancements can be made. Promising approaches include windowing schemes to smooth the time-domain symbol transitions are widely studied. The WOLA-OFDM [7] has been intensively discussed along this line of study, and schemes have been proposed for asynchronous 5G [32], [33]. Indeed, a large part of OOB emission of CP-OFDM comes from the discontinuity between adjacent symbols. A natural and straightforward way to reduce the OOB emissions is to avoid the conventional usage of rectangular pulse shape, and a one with soft edges is used instead to smooth the transition between adjacent symbols. These soft edges are added to the cyclic extensions of a given symbols by a time domain windowing [32]. More specifically, the windowing operation can be performed on both the original cyclic prefix and the newly added cyclic suffix. To create this latter, we copy and append the first W_{Tx} samples of a given symbols to its end. Adjacent symbols could overlap with each other in the edge transition regions, which leads to a similar overhead as in the classical CP-OFDM. In addition to the transmit windowing, an advanced receive windowing is applied to suppress the asynchronous inter-user interference (i.e. adjacent non-orthogonal signals). It contains two steps. In the first step, the receiver takes $N_{\text{FFT}} + 2W_{Rx}$ samples (N_{FFT} denotes the FFT size), which correspond to the samples of one WOLA-OFDM symbol. Then, these samples are windowed. In the second step, an Overlap and Add processing [33] is applied to create the useful N_{FFT} samples from the $N_{\text{FFT}} + 2W_{Rx}$ ones.

2) UF-OFDM (WF03)

UF-OFDM has recently been proposed by Alcatel-Lucent Bell Laboratories [15], and it is also referred to UF-OFDM in the literature [34]. UF-OFDM is a combination of ZP-OFDM (traditional CP-OFDM where the CP is replaced by a Zero Padding (ZP) [35]) and filtered-OFDM which is further detailed in Section II-B.3: each OFDM symbol at the output of the IFFT is filtered and the ZP is used to absorb the filter transient response. In the absence of a multipath channel, UF-OFDM holds the orthogonality of the subcarriers. Nevertheless, the orthogonality is no longer sustained as the time spreading of the channel increases and only provides a soft protection against multipath effects at the receiver.

At the reception, the multiuser interferences coming from time and frequency asynchronism are first reduced by applying a window on the received UF-OFDM block symbols [36]. This windowing is similar to the one used for WOLA-OFDM described in Section II-B.1. It has to be noted that windowing destroys the subcarrier orthogonality even if the channel is perfect. Finally, a FFT of size two times greater than the IFFT used at the transmission is applied to the received UF-OFDM block symbols and only even subcarrier indexes are kept. It is important to note that the complexity of the receiver can be reduced by collecting additional samples corresponding to the length of the ZP and using an overlap-and-add method to obtain the circular convolution property [35]. In this case, the required FFT size is identical to the size of the IFFT used at the transmission. All existing and already developed OFDM-based designs are applicable to UF-OFDM such as MIMO, channel estimation/equalization, pilot, synchronization, PAPR reduction (DFT precoding or any others approaches).

3) FILTERED-OFDM (WF04)

f-OFDM has been recently proposed as a 5G candidate at the 3GPP RAN1 workgroup [37]. This scheme is based on traditional CP-OFDM and follows a pragmatic approach to overcome problems raised by the use of asynchronous communications for which traditional CP-OFDM is known to provide poor performance. At the transmission, the poor out-of-band radiation of traditional CP-OFDM is improved using a filter at the output of a CP-OFDM transmitter. At the reception, the interferences coming from time and frequency asynchronous adjacent users are lowered thanks to a similar filter at the input of a CP-OFDM receiver. As for UF-OFDM, all existing and already developed OFDM-based designs are applicable to f-OFDM. The filtering process required by f-OFDM generates inter block interferences, but if the filter is properly designed the impact of these interferences on the link performance are negligible [37]. It has to be noted that the ramp-up and the ramp down generated by the filter increase the burst length, and consequently the latency and reduce the spectral efficiency . A pragmatic approach [37] consists in hard truncating at both burst edges with an appropriate length in order to reduce the burst size. Since burst tails are very well localized in time, this truncation generates limited out-of-band emission. Both simulations and [37] show that a truncation length equals to half the CP length provides good performance in the case of a LTE scenario.

4) N-CONTINOUS OFDM (WF05)

The N-continuous OFDM scheme has been introduced for the first time in [9]. Basically, the idea consists in creating consecutive adjacent OFDM symbols which are continuous in the time domain in order to improve the poor out of band radiation of traditional CP-OFDM. The construction of OFDM symbols will render the transmitted signal and its first N derivatives continuous using a precoding matrix which is placed between the symbol mapping and the IFFT. One advantage of N-continuous OFDM scheme is to have traditional CP-OFDM as its core WF at both transmission and reception. Nevertheless, in its basic form, this scheme requires the transmission of side information (precoding matrix) to the receiver in order to recover the data. A solution to cope with this problem has been proposed in [38] and consists in using a systematic precoding matrix at the price of an increase of the transmitted signal quality (e.g. Error Vector Magnitude (EVM)).

5) FMT (WF06)

FMT is a multicarrier modulation technique that has been specifically developed for DSL applications [14]. In FMT, a conventional method of frequency division multiplexing is used, i.e. the subcarrier bands are juxtaposed. Each band can be seen as a traditional single carrier modulation which respects the Nyquist criteria. It is well known that the optimal repartition (in terms of Signal to Noise Ratio at the demodulation input) of the Nyquist filter is a square-root Nyquist filter at both emission and reception sides. Square root Nyquist filters limit the effective transmission bandwidth of each band to $B = (1+\alpha) \cdot F_s$, where F_s is the sampling frequency and α is the excess bandwidth coefficient (also called roll off factor). The use of a $\alpha > 0$ can be seen as suboptimal since the spectral efficiency decreases by the same amount. One can imagine that small α is a good solution, but the time/frequency duality requires large square root Nyquist filter length which drastically increases the latency and the overhead. Some recent works have proposed new filters [39] in order to cope as much as possible with this problem providing a good compromise between out of band radiation and group delay. FMT transmitter and receiver can be efficiently implemented using polyphase filter and (I)FFT [40] only if the spacing between subcarrier is fixed (which is usually the case).

6) FFT-FBMC (WF07)

In order to overcome the FBMC intrinsic interference issue, FFT-FBMC scheme, together with a special data transmission strategy has been proposed in [17] and [41]. This scheme proceeds by precoding the data in a subcarrier-wise manner using an IFFT. Thus, the interference coming from the same subcarrier is removed by a simple equalization thanks to the subcarrier-wise IFFT/FFT precoding/decoding and CP insertion. Whereas the interference coming from the adjacent subcarriers can be avoided by a special data transmission strategy and a good frequency-localized prototype filter.

In FFT-FBMC proposal, blocks of $N/2$ data complex symbols in each subcarrier k go through a N-IFFT operation. After that, the N-IFFT outputs are optionally extended with a CP, and fed to the M-FBMC modulator in a given carrier k. At the output of the FBMC demodulator, the serial symbols in a given subcarrier q are converted to parallel blocks, and if needed the CP is discarded to only keep N symbols in each block. After that, each block is fed to a N-FFT whose only $N/2$ output symbols are kept for detection.

The intercarrier interference is avoided thanks to the $N/2$ zeros inserted in the N-IFFT in each subband. That is, the $N/2$ zeros inserted in each N-IFFT serve to isolate the adjacent subbands [42]. Thus, the complex orthogonality is guaranteed in FFT-FBMC. It is shown in [43] that single-tap equalization can be performed. The equivalent channel coefficients are the $MN/2$ channel frequency response coefficients weighted by coefficients depending on the used prototype filter.

7) BF-OFDM (WF08)

Block-Filtered OFDM (BF-OFDM) is another precoded filter-bank multi-carrier modulation [16], [44]. The precoding scheme is performed by means of CP-OFDM modulators (of size N) and the filtering operation is applied with a PolyPhase network (PPN) (of size M) as for FFT-FBMC introduced in Section II-B.6. However, the main difference with respect to the latter WF is the insertion of a filter pre-distortion stage at the transmitter side. The extra stage aims at compensating the distortion induced by the filter so as to flatten the transmitted signal spectrum inside the carrier bandwidth. As a consequence, no filtering stage is required at the receiver side to properly recover the signal and the receiver scheme can be reduced to a simple $\frac{MN}{2}$-FFT preceded by a CP removal.

C. WFs WITH REAL ORTHOGONALITY

1) FBMC-OQAM (WF09)/Lapped-OFDM (WF10)

Despite the large success of CP-OFDM as the multicarrier benchmark, it has to deal with the many requirements envisaged in future generation physical layer. Indeed, the capability of using non-contiguous spectrum with a relaxed synchronization are the main challenges of the desired future WF that OFDM cannot fulfill. In fact, the poor localized frequency response of rectangular transmit filter of CP-OFDM induces high level of OOB radiation. Besides, the rectangular receive filter also brings an important amount of interference from other asynchronous users [21]. In order to overcome the main OFDM shortcomings, FBMC systems have been proposed as an alternative to OFDM offering better frequency localization and flexible access to the available resources.

The key-idea of FBMC is to use well-frequency localized prototype filters, instead of the OFDM rectangular one, providing thus better adjacent channel leakage performance compared to OFDM. In order to ensure orthogonality between adjacent symbols and adjacent subcarriers, while keeping maximum spectral efficiency, Nyquist constraints on the prototype filter combined with OQAM are used. Indeed, in OQAM, the in-phase and the quadrature components of a given QAM symbol are time staggered by half a symbol period, $M/2$ (i.e. $T/2$). The duration of the prototype filters is usually a multiple of the FFT size ($L = KM$), where K is called the overlapping factor. In this paper, we consider two cases:

- FBMC-OQAM: using the most commonly used PHYDYAS filter [45] with $K = 4$.
- Lapped-OFDM: using the sine prototype filter with $K = 2$. It is worth noticing that the name of this WF is derived from the lapped orthogonal transform. Interested readers are referred to [11] for more details.

2) WCP-COQAM (WF11)

Despite the various advantages of FBMC systems, the long prototype filters could be questionable for low-latency communications [46]. Besides, FBMC signals are not suitable to short packet transmission due to long ramp-up/down of FBMC signal leading thus to a non-negligible loss in spectral efficiency. In order to overcome this situation, burst truncation can reduce this loss but it has detrimental effects like additional interference and significant OOB radiation [47]. Circular convolution with time-windowing was proposed in [12] and [48] to remove the overhead signal while maintaining smooth transition at the burst edges. This solution is known as Windowed Cyclic Prefix-based Circular-OQAM (WCP-COQAM). In order to avoid multipath channel interference, a CP can easily be inserted since COQAM corresponds to a block transform [48]. Thanks to circular convolution, the continuity of CP-COQAM signal is maintained inside a given CP-COQAM block. However, since signal discontinuities can be observed between different CP-COQAM blocks, there is no remarkable difference between the CP-COQAM spectrum and CP-OFDM one [21]. Note that this behavior is independent of how well is localized the prototype filter frequency response. Accordingly, a windowing is necessary to reduce the significant OOB radiation induced by inter-block discontinuities. In the receiver side, the CP is removed, windowed samples are compensated and the receive circular convolution is applied afterwards. The OQAM decision is then made to recover the desired useful data symbols.

D. WFs WITHOUT ORTHOGONALITY

1) FBMC-QAM (WF12)

As previously discussed, filter-bank based WFs use a per-subcarrier filtering, reducing thus out-of-band emission and providing more flexibility to meet the future physical layer requirements. As emphasized earlier, such enhancements are at the price of orthogonality condition that only holds in the real domain and is no longer valid in the presence of practical channels. Indeed, the self-interference inherent to OQAM-based schemes is a major problem when considering MIMO STBC/SFBC [49] or spatial multiplexing with maximum likelihood detection [50]. Some solution schemes were proposed based on iterative interference estimation and cancellation. However, such solutions are limited by error propagation induced by the residual interference since the interference power is as strong as the useful signal power [10], [51]. In order to overcome this problem, it has been demonstrated, in [52] and [53], that the interference power must be small and should be kept under a certain threshold, in order to counteract the error propagation phenomenon and consequently make more efficient the

interference cancellation scheme. In order to achieve this objective and reduce the interference level, the authors in [51] were the first to propose the utilization of QAM modulation, instead of OQAM one, in FBMC systems. Actually, a significant part of self-interference is avoided by only transmitting QAM symbols every signalling period $nT, n \in \mathbb{Z}$. In other words, the interference induced by OQAM symbols transmitted in $(2n+1)\frac{T}{2}, n \in \mathbb{Z}$ is no longer considered [50]. Such a combination is called FBMC-QAM systems. In order to improve the performance of FBMC-QAM symbols, new prototype filters have been designed, optimizing simultaneously spectrum localization, self-interference level, and overall spectral efficiency [13]. In this paper, we consider one of these prototype filters which that we call 'Samsung Type-I'. Thanks to the latter, the signal to interference ratio (SIR) is twice that of PHYDYAS case. Interested readers are referred to [13] for more details.

2) GFDM (WF13)

Generalized Frequency Division Multiplexing (GFDM) is a WF performing a time-frequency filtering over data block [18]. The WF is therefore flexible but also non-orthogonal.

A data block corresponds to the set of symbols transmitted over a group of N_A consecutive sub-carriers over N_B time slots and thus is composed of $N_T = N_A \times N_B$ symbols. The sub-carrier wise filtering is performed by means of circular convolution. However, as the symbols overlap in both time and frequency, interference (inter and intra data blocks) is generated. It is worth noticing that inter data block interference can be avoided by proper dimensioning of the CP. Moreover, in order to improve the side lobe rejection, a windowing is applied at the transmitter side. However, this process increases the interference level that can be mitigated at the receiver side with a tail biting approach [18].

In the litterature two receiver schemes has prevailed: the Matched Filter (MF) and the Zero-Forcing (ZF) architectures [54]. With the MF approach, the received blocks are filtered by the transmission matched filters. This scheme provide low complexity but poor performance due to inter-symbol interference (ISI). ISI cancellation scheme can be considered in order to improve the performance at the expense of significant complexity increase [55]. When it comes to the ZF approach, the signal is demodulated with the Moore pseudo-inverse of the transmitter matrix. This scheme suffers from noise enhancement and the provided performance depends on the properties of the transmitter matrix [56].

The block diagrams of the transmitter/receiver of all considered WFs are shown in Fig. 1

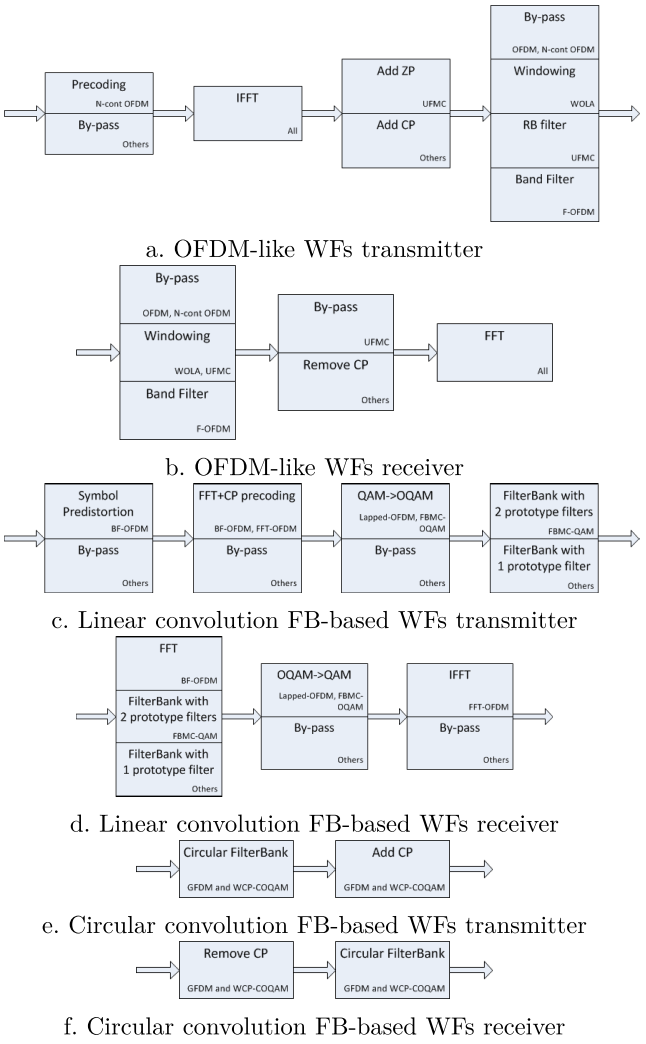

FIGURE 1. WFs block diagrams. (a) OFDM-like WFs transmitter. (b) OFDM-like WFs receiver. (c) Linear convolution FB-based WFs transmitter. (d) Linear convolution FB-based WFs receiver. (e) Circular convolution FB-based WFs transmitter. (f) Circular convolution FB-based WFs receiver.

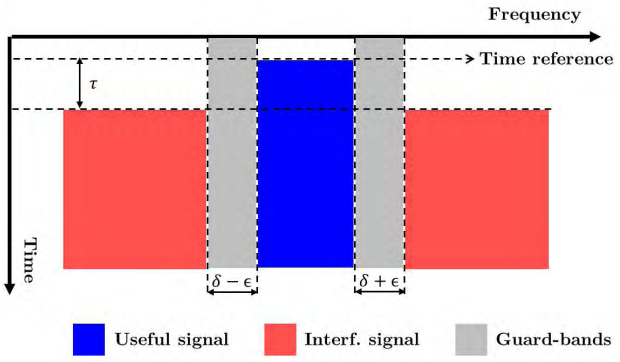

FIGURE 2. Coexistence scenario: two asynchronous users with τ [s] TO, ϵ [kHz] CFO and free guard-bands of δ [kHz].

III. SYSTEM MODEL

A. COEXISTENCE SCENARIO

In this study, we consider a scenario of two coexisting users sharing the available frequency band as depicted in Fig. 2, where the blue colored area and the red colored one correspond to the time/frequency resources allocated to the user of interest and the other one, respectively. The useful

TABLE 2. General parameters.

General	
RB bandwidth	180 kHz
Useful bandwidth of user of interest (UOI)	540 kHz
Interfering bandwidth	2×1.62 MHz
TO (τ)	[-33.33,+33.33]μs
CFO (ε)	[-1.5,+1.5]kHz
Input data	16-QAM
Guard-band δ	[0, 75] kHz

signal occupies a frequency band of 540 kHz equivalent to 3 LTE RB (LTE-RB bandwidth = 180 kHz) while 1.62 MHz (i.e. 9 LTE-RB) are allocated to the other user on each side of the useful frequency band. A guard-band of δ kHz , illustrated by a gray colored area, is separating the frequency bands of both users. Several cases are considered for guard-bands: no guard band, 15 kHz, 45 kHz and 75 kHz.

The receiver of interest is assumed to be perfectly synchronized, in both time and frequency domains (i.e. neither Timing Offset (TO) nor Carrier Frequency Offset (CFO) are considered), and is situated at equal distance from both transmitters.[1] However, as illustrated in Fig. 2, a time/frequency synchronization misalignment (τ and ε denote timing and carrier frequency offsets, respectively) can occur between the receiver of interest and the other user. Note that we consider a TO distributed between $-T/2$ and $+T/2$, where T is the OFDM symbol duration ($T = 66.66\mu s$). Due to this synchronization mismatch, the receiver of interest potentially suffers from the interference inducing thus performance degradation. It is worth mentioning that the CFO induces a shift of both red-colored areas of the interfering signal spectrum by ε kHz where the resulting guard bands become $\delta - \varepsilon$ kHz on one side and $\delta + \varepsilon$ kHz on the other side. In order to highlight the impact of this interference, we consider free-distortion channels (perfect and noiseless channels) between both transmitters on one side and the victim receiver on the other side.

B. PARAMETERS

In this section, we provide the general parameters of the scenario previously described (see Table 2) as well as specific parameters related to the different WFs considered in this document:

- WFs with complex orthogonality: Table 3,
- WFs with real orthogonality: Table 4,
- Non-orthogonal: Table 5.

IV. WAVEFORM COMPARISON

This section is devoted to compare the performance of the WF candidates described in Section II in terms of:

- Power Spectral Density (PSD): the out-of-band radiation of the interfering signal is evaluated.

[1]Note that in this work, we assume the same transmit power per subcarrier for both useful and interfering users

TABLE 3. WFs with complex orthogonality.

CP-OFDM	
FFT size (N_{FFT})	1024
CP length (N_{CP})	72
Subcarrier spacing	15 kHz
Sampling Frequency (F_s)	15.36 MHz
WOLA-OFDM	
FFT size (N_{FFT})	1024
CP length (N_{CP})	72
Windowing	Raised cosine
W_{Tx},W_{Rx}	$(20, 32)$
Subcarrier spacing	15 kHz
Sampling Frequency (F_s)	15.36 MHz
UF-OFDM	
FFT size (N_{FFT})	1024
Filter	Dolph-Chebyshev
Filter length	73 ($\mathrm{L_{FIR}}$ =ZP+1)
Zero padding length (N_{ZP})	72
Stop-band attenuation	40 dB
Receive windowing	Raised cosine
Receive windowing size	36
Subcarrier spacing	15 kHz
Sampling Frequency (F_s)	15.36 MHz
f-OFDM	
FFT size (N_{FFT})	1024
Filter	the same at both Tx and Rx
Filter length	512
CP length (N_{CP})	72
Transition band	2.5×15 kHz
Burst truncation	$N_{\mathrm{CP}}/2$ on each side
Subcarrier spacing	15 kHz
Sampling Frequency (F_s)	15.36 MHz
N-Continuous OFDM	
FFT size (N_{FFT})	1024
CP length	72
Continuity order	2 (second derivative)
Precoding matrix knowledge at Rx	none
Subcarrier spacing	15 kHz
Sampling Frequency (F_s)	15.36 MHz
FMT	
Filter	[39]
Roll-off factor α	0.25
Overlapping factor (K)	16
FFT size (N_{FFT})	$(1+\alpha)1024$
Filter length	KN_{FFT}
Subcarrier spacing (F_s)	15 kHz
Sampling Frequency	15.36 MHz
BF-OFDM / FFT-FBMC	
M	64
N	64
K	4
BF-OFDM Rx FFT size	2048
CP size	4
Carrier bandwidth	180 kHz
Sampling Frequency	11.52 MHz
Prototype Filter	Gaussian (BT=0.33)

- Spectral efficiency function of the number of transmitted symbols per frame.
- End-to-End Physical layer latency (E2E): corresponds to the time delay between the transmission of a given information and the recovery of the latter.
- Time and frequency synchronization errors between the interfering transmitter and the receiver of interest.
- Power fluctuation: Instantaneous-to-Average Power Ratio (IAPR) is analyzed.

TABLE 4. WFs with real orthogonality.

FBMC-OQAM	
Prototype Filter	PHYDYAS
Overlapping factor (K)	4
FFT size (N_{FFT})	1024
Subcarrier spacing	15 kHz
Sampling Frequency (F_s)	15.36 MHz
Lapped-OFDM	
Prototype Filter	sinus
Overlapping factor (K)	2
FFT size (N_{FFT})	1024
Subcarrier spacing	15 kHz
Sampling Frequency (F_s)	15.36 MHz
WCP-COQAM	
CP length N_{CP}	72
Transmit windowing	Raised cosine
Window length (W_{Tx})	20
Prototype Filter	PHYDYAS
Overlapping factor (K)	4
FFT size (N_{FFT})	1024
Subcarrier spacing	15 kHz
Sampling Frequency (F_s)	15.36 MHz

TABLE 5. Non orthogonal WFs.

FBMC-QAM	
Prototype Filter	Samsung Type I [13]
Overlapping factor (K)	4
FFT size (N_{FFT})	1024
Subcarrier spacing	15 kHz
Sampling Frequency (F_s)	15.36 MHz
GFDM	
FFT size (N_A)	1024
CP length (N_{CP})	72
Block size (N_B)	7
Subcarrier spacing	15 kHz
Sampling Frequency (F_s)	15.36 MHz

- Transceiver complexity: only the number of multiplications per unit of time of modulation/demodulation process is considered.

A. POWER SPECTRAL DENSITY

It is well established that traditional CP-OFDM has poor frequency domain localization. For instance, LTE system requires the use of 10% of the system bandwidth as guard bands. These large guard bands located at both edges of the spectrum are necessary in order to reach enough attenuation to meet LTE spectrum mask requirement. It is expected that future 5G systems use more efficiently the allocated bandwidth and large guard bands can be seen as a waste of spectral efficiency. Thus, good or excellent spectral containment will be a key parameter for future 5G WF in order to support neighboring and non orthogonal signals.

We present in Fig. 3 the PSD (Power Spectral Density) comparison of the considered WFs. We choose to plot only the contribution of the interference users so that we can observe at the same time the level of out-of band emission and the level of emission within a spectral hole. As expected, the worst PSD performance is given by the traditional CP-OFDM WF. The far-end PSD is dominated by the WFs which have their filtering applied to each subcarrier, namely Lapped-OFDM, FBMC-QAM, FBMC-OQAM and FMT.

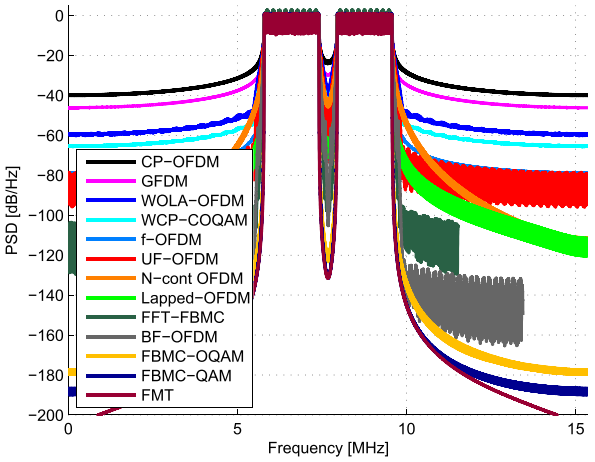

FIGURE 3. Interference users PSD comparison.

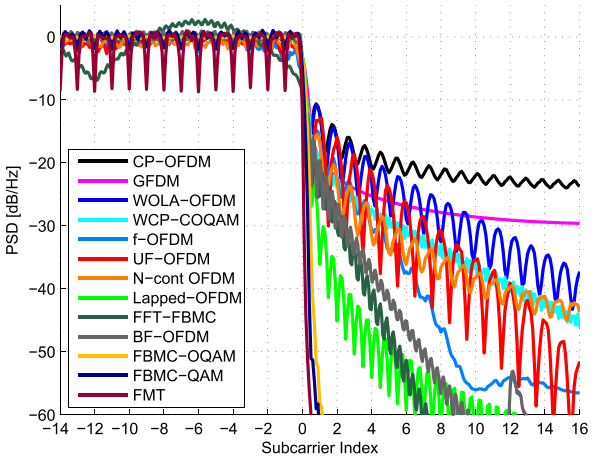

FIGURE 4. Comparison of the interference users PSD edge according to the subcarrier index.

BF-OFDM and FFT-FBMC provide also excellent PSD performances thanks to the use of the filterbank approach in the signal construction. N-continuous OFDM has a relatively slow decaying but provides good far-end PSD. UF-OFDM and f-OFDM apply a filter to a group of subcarriers and we can observe that their performances are in the same order of magnitude. WCP-COQAM presents moderate far-end PSD performance due to time domain transition between successive blocks. The time domain windowing applied to transmitted OFDM blocks (WOLA-OFDM) improves by about 20 dB the performance of traditional CP-OFDM, but its far-end PSD performance remains moderate. Similar to WCP-COQAM, GFDM is not very well localized in the frequency domain due to the block construction of GFDM signal generating time domain transitions between blocks.

In Fig. 4, we present a zoom of the PSD at one edge of the spectrum in function of the subcarrier index.[2] Again, the WFs which have their filter applied to each subcarrier provide

[2]Note that the subcarrier spacing is set to 15 kHz since all considered waveforms, except FFT-FBMC and BF-OFDM, have the same value. The subcarrier spacing of FFT-FBMC and BF-OFDM is about three times lower, i.e. 5.625 kHz, in the considered parameterization.

TABLE 6. Spectral efficiency and End-to-End Physical layer latency comparisons.

WF	Spectral Efficiency	Asymptotic Spectral Efficiency	End-to-End Physical layer latency
OFDM	$\frac{N_{\text{FFT}}}{N_{\text{FFT}}+N_{CP}}$	$\frac{N_{\text{FFT}}}{N_{\text{FFT}}+N_{CP}}$	$S \times \frac{N_{\text{FFT}}+N_{CP}}{F_s}$
WOLA-OFDM	$\frac{S\times N_{\text{FFT}}}{S\times(N_{\text{FFT}}+N_{CP})+W_{\text{Tx}}}$	$\frac{N_{\text{FFT}}}{N_{\text{FFT}}+N_{CP}}$	$\frac{S\times(N_{\text{FFT}}+N_{CP})+W_{\text{Tx}}}{F_s}$
UF-OFDM	$\frac{N_{\text{FFT}}}{N_{\text{FFT}}+ZP}$	$\frac{N_{\text{FFT}}}{N_{\text{FFT}}+ZP}$	$S \times \frac{N_{\text{FFT}}+L_{\text{ZP UF-OFDM}}}{F_s}$
f-OFDM	$\frac{S\times N_{\text{FFT}}}{S\times(N_{\text{FFT}}+N_{CP})+L_{\text{Trunc}}}$	$\frac{N_{\text{FFT}}}{N_{\text{FFT}}+N_{CP}}$	$\frac{S\times(N_{\text{FFT}}+N_{CP})+L_{\text{Trunc}}}{F_s}$
N-Cont OFDM	$\frac{N_{\text{FFT}}}{N_{\text{FFT}}+N_{CP}}$	$\frac{N_{\text{FFT}}}{N_{\text{FFT}}+N_{CP}}$	$S \times \frac{N_{\text{FFT}}+N_{CP}}{F_s}$
FMT	$\frac{S}{(S+K-1)(1+\alpha)}$	$\frac{1}{1+\alpha}$	$\frac{(S-1+K)N_{\text{FFT}}}{F_s}$
FFT-FBMC	$\frac{S\times\frac{N}{2}}{K+\frac{1}{2}[S\times(N+N_{CP})-1]}$	$\frac{N}{N+N_{CP}}$	$\frac{M\times\frac{N}{2}\times S+M\times\frac{N_{CP}}{2}\times(S-1)+\left[(N_{CP}-3)\times\frac{M}{4}+K\times\frac{M}{2}\right]}{F_s}$
BF-OFDM	$\frac{S\times\frac{N}{2}}{K+\frac{1}{2}[S\times(N+N_{CP})-1]}$	$\frac{N}{N+N_{CP}}$	$\frac{\frac{M}{2}\left[S\times N+N_{CP}(S-1)+\frac{N_{CP}-3}{2}+K\right]}{F_s}$
FBMC-OQAM	$\frac{S}{S+K-1/2}$	1	$N_{\text{FFT}}\frac{S-\frac{1}{2}+K}{F_s}$
Lapped-OFDM	$\frac{S}{S+3/2}$	1	$\frac{S+\frac{3}{2}}{F_s}$
WCP-COQAM	$\frac{KN_{\text{FFT}}}{KN_{\text{FFT}}+N_{CP}}$	$\frac{KN_{\text{FFT}}}{KN_{\text{FFT}}+N_{CP}}$	$S \times \frac{KN_{\text{FFT}}+N_{CP}}{F_s}$
FBMC-QAM	$\frac{S}{S+K-1}$	1	$N_{\text{FFT}}\frac{S-1+K}{F_s}$
GFDM	$\frac{N_B\times N_{\text{FFT}}}{N_B\times N_{\text{FFT}}+N_{CP}}$	$\frac{N_B\times N_{\text{FFT}}}{N_B\times N_{\text{FFT}}+N_{CP}}$	$S\frac{N_B\times N_{\text{FFT}}+N_{CP}}{F_s}$

the best PSD performance: FBMC-QAM, FBMC-OQAM and FMT provide an extremely fast spectrum decaying and only one subcarrier spacing is necessary to achieve very low PSD levels. Nevertheless, and due to shorter prototype filter duration ($K = 2$), Lapped-OFDM has lower spectrum decaying than the aforementioned WFs. FFT-OFDM and BF-OFDM are efficient WFs thanks to their (almost) linear decaying at the horizon of few subcarriers. For instance, they respectively requires 4 and 5 (15 kHz) subcarriers to achieves an attenuation of 40 dB. It is interesting to note that FFT-OFDM shows some slight ripples within the useful bandwidth (periodicity of 180 KHz or 1 RB) due to the frequency response of the prototype filter. On the other hand, the BF-OFDM symbol preditortion efficiently pre-compensates this effect. The PSD of f-OFDM requires few subcarriers to be drastically improved with respect to traditional CP-OFDM due to the transition bandwidth of the filter which has been set to $\partial W = 2.5$ subcarriers. Finally, all other WFs provides moderate performance and requires more than one resource block (12 subcarriers) to reach an attenuation of -40 dB.

B. SPECTRAL EFFICIENCY AND LATENCY

Spectral efficiency (SE) given in bits/s/Hz is a key parameter for high data rate systems since it gives a clear idea of achievable data rates for a given bandwidth. In Table 6, we present the SE according to the number of transmitted parallel vector symbols S, and also its asymptotic version called Asymptotic Spectral Efficiency (ASE) where S tends toward infinity. Note that we do not include the impact of the constellation dimension since it is supposed to be identical for all WFs. The required number of parallel vectors is different for each WF and depends on the number of complex QAM symbols N_{QAM} to be transmitted, but also on the way a block symbol is built. S is given by:

$$S = \begin{cases} \lceil \frac{N_{QAM}}{K \times N_A} \rceil & \text{for WCP-OQAM} \\ \lceil \frac{N_{QAM}}{N_B \times N_A} \rceil & \text{for GFDM} \\ \lceil \frac{N_{QAM}}{M_A \times \frac{N}{2}} \rceil & \text{for FFT-FBMC and BF-OFDM} \\ \lceil \frac{N_{QAM}}{N_A} \rceil & \text{otherwise} \end{cases}$$

where $\lceil . \rceil$ refers to the ceiling operation, and N_A and M_A are respectively the number of used subcarriers and the number of active carriers (for FFT-OFDM and BF-OFDM). We can observe that for small values of S, the WFs which have their filter applied to each subcarrier have a spectral efficiency penalty due to their longer impulse response. This is especially true for FMT since the overlap factor K is usually much longer: for instance we usually consider $K = 16$ for a roll off factor of 0.25, instead of $K = 2$ for Lapped-OFDM or $K = 4$ for FBMC-OQAM and FBMC-QAM. All the WFs which require a guard interval (CP or ZP) suffer from the fact that this guard interval does not transmit any useful information. When S tends toward infinity, only FBMC derivatives (Lapped-OFDM, FBMC-OQAM and QAM) achieve full capacity, i.e. ASE=1.

The latency of a WF is also another key parameter, especially when considering very low response systems such as in tactile Internet scenarios. In this article, we use the End-to-End Physical layer latency criterion (E2E) defined as the time delay from which the FEC (Forward Error Correction) is capable to decode the bits corresponding to the N_{QAM} transmitted symbols. In other words, it refers to the time between the availability of the bits at the output of the FEC at the transmitter side, and the beginning of the channel

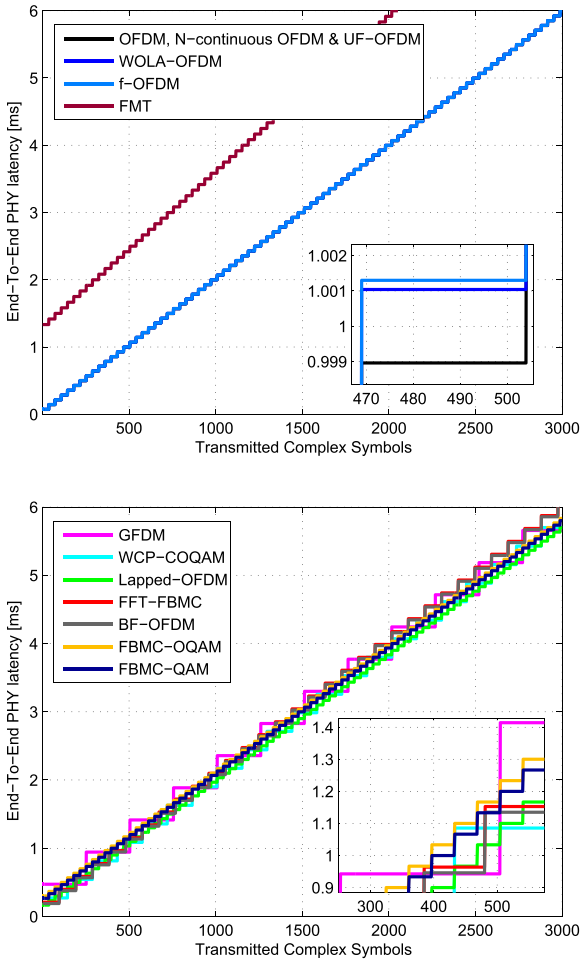

FIGURE 5. End-to-End Physical Layer latency (in ms) for WFs with complex orthogonality (up), and for the other considered WFs (down) according to the number of transmitted N_{QAM} symbols for a user using 3 RB.

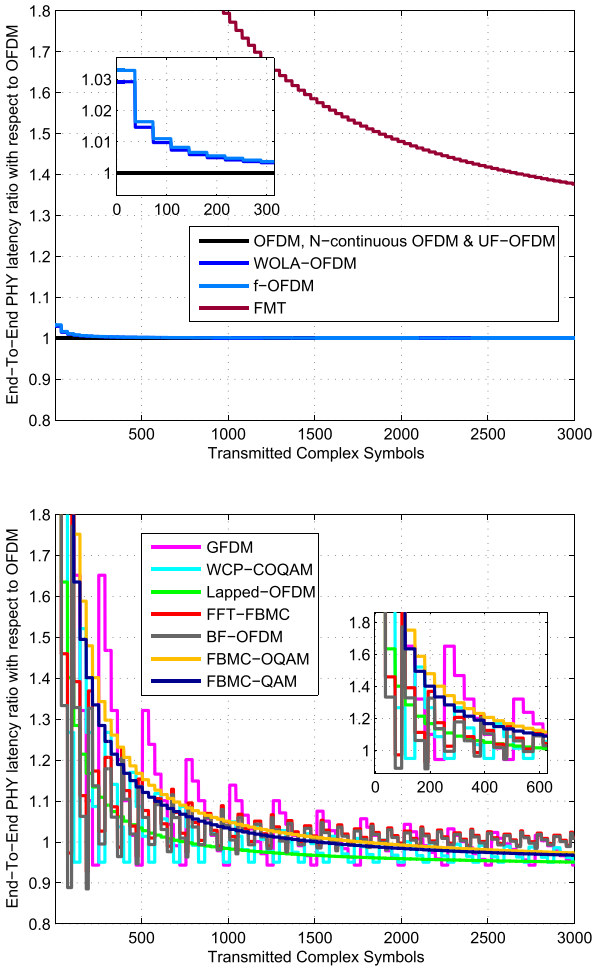

FIGURE 6. End-to-End Physical layer latency ratio for WFs with complex orthogonality (up), and for the other considered WFs (down) with respect to traditional CP-OFDM scheme for a user which used 3 RB.

decoding at the receiver side. Thus, it is important to note that E2E does not take into account the processing time required by channel coding and decoding or equalization because it is implementation and design dependent. The potential delay introduced by the channel is also not considered. E2E comparison is provided by Table 6 and is also graphically presented in Fig. 5 according to N_{QAM} and for a user which uses 3 RB corresponding to $3 \times \frac{N}{2} = 96$ subcarriers for FFT-FBMC and BF-OFDM, and $N_A = 3 \times 12 = 36$ subcarriers for all other considered WFs. In this Fig., we can observe that the large group delay of the FMT prototype filter and the loss of spectral efficiency due to the roll off factor drastically increase the latency of FMT scheme. All other WFs latencies are in the same order of magnitude. In order to better assess the performance of the other WFs, we present in Fig. 6 the E2E with respect to traditional CP-OFDM scheme. We can observe that for small N_{QAM} values, the latencies are in general (much) greater than traditional OFDM, and there exist only few WFs and few settings which provide better performance. When N_{QAM} increases, FBMC derivative WFs become a little bit better than OFDM, and the other WFs have much more settings which give better latency performance.

C. ASYNCHRONOUS ACCESS

In this section, as mentioned previously, we discuss the performance of the considered WFs in multi-user asynchronous access. In order to focus on the asynchronous interference impact on the performance of various WF schemes, we propose to measure the normalized mean square error (MSE)[3] on the decoded symbols (of the user of interest) in ideal noiseless channel. Note that normalized MSE is adopted since it is independent of the constellation scheme. Both per-subcarrier MSE and average MSE are assessed vs. TO or Carrier Frequency Offset (CFO). Actually, per-subcarrier MSE can provide a meaningful information about the distribution of asynchronous interference across useful subcarriers. Two cases of guard-bands are examined: $\delta = 0$ and 75 kHz. Note that for the per-subcarrier MSE figures, we use a color map indicating the MSE levels: from dark blue color when the MSE is less than or equal to -40dB to dark red color when the MSE is greater than or equal to -10dB.

[3]The normalized MSE is computed by dividing the MSE by the average power of the signal constellation

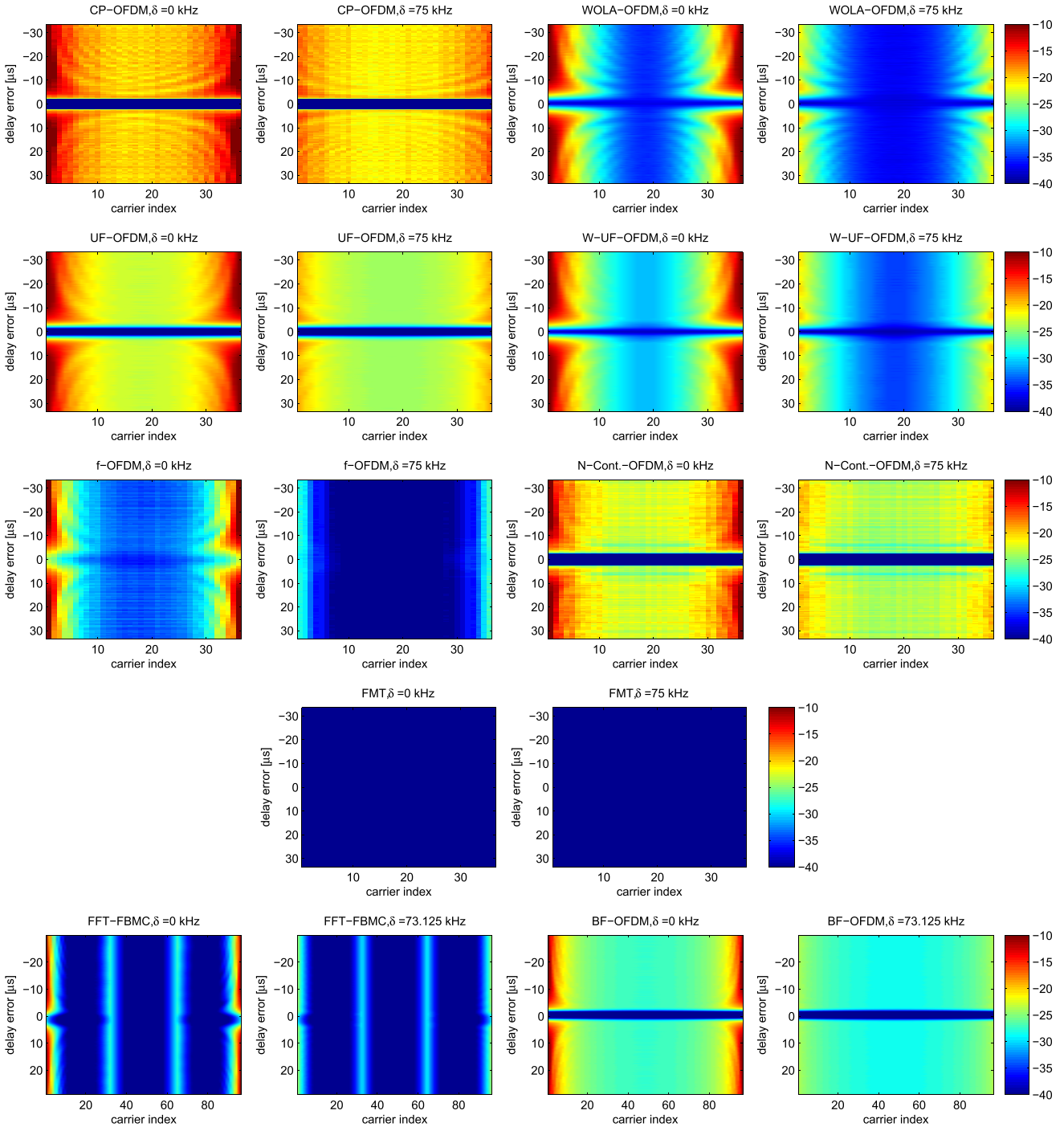

FIGURE 7. WFs with complex orthogonality: per-subcarrier NMSE against TO, $\delta = 0$ and 75kHz (73.125kHz for FFT-FBMC and BF-OFDM).

1) TIMING OFFSET

In order to distinguish the degradation induced by timing synchronization errors from the one caused by CFO, we consider in this section that there is no CFO ($\varepsilon = 0$ Hz) between the interfering signal and the useful one. The timing misalignment τ varies from $-33.33\mu s$ to $+33.33\mu s$.

a: WFs WITH COMPLEX ORTHOGONALITY

The per-subcarrier MSEs of WFs with complex orthogonality are depicted in Fig. 7.

In CP-OFDM case, we can distinguish two regions: when $|\tau| < N_{CP}/2$, we observe a dark blue region (MSE below -40 dB) which means that there is no asynchronous interference. Such a result is due to the fact that the orthogonality

between subcarriers is maintained as long as the delay error τ does not exceed the CP duration. When τ is outside the CP interval, the orthogonality is no longer ensured. This loss of orthogonality gives rise to a strong level of asynchronous interference. We can see that the interference level slowly decreases as the spectral distance between the victim subcarrier and the interfering ones increases. Similarly, we observe a negligible enhancement when increasing the guard band. Such a behavior is due to the poor frequency localization of the rectangular transmit/receive OFDM filters.

We move now to WOLA-OFDM, where additional remarks can be made. The interference level in the middle of the bandwidth becomes lower (approx. -35 dB) compared to CP-OFDM scheme. We can also see that blue colored area (MSE less than -30 dB) becomes larger when increasing the guard band. This can be explained by the fact that the WOLA processing applied at the receiver is able to suppress inter-user interference as well. Indeed, when users are not synchronized, the soft edges applied at the receiver help to reduce inter-user interference resulting from the mismatched FFT capture window.

Thanks to the per-RB filtering, the UF-OFDM scheme shows better performance compared to CP-OFDM. However, the gain achieved by UF-OFDM remains marginal. Moreover, thanks to additional windowing at the receiver side, W-UF-OFDM offers a higher gain compared to the basic scheme of UF-OFDM when the TO is outside the ZP region. Similar to WOLA-OFDM, the ZP region offering the lowest MSE is significantly reduced in W-UF-OFDM because the ZP length is originally used to absorb the transmit filter response. Furthermore, when increasing the spectral distance of the victim subcarrier from the interfering ones, the interference level decay is more important compared to CP-OFDM but less significant when compared to WOLA-OFDM.

In the f-OFDM scheme, since filtering is applied at both transmitter and receiver sides, the inner subcarriers are more protected compared to the previous schemes. In fact, the long filters used in this WFs offers a better frequency localization of the transmitted signals and a better protection against inter-user interference compared to WOLA-OFDM and W-UF-OFDM. However, it is worth pointing out the fact the CP is completely used to absorb only a part of the transmit/receive filters responses.

Concerning the N-cont. OFDM WF, one can see that the MSE is almost the same as in UF-OFDM case when TO exceeds the CP region. Inside this region, the orthogonality between subcarriers is maintained as in CP-OFDM case leading thus to the absence of asynchronous interference. It is worth pointing out that N-cont. OFDM version presented in this article intentionnaly creates high level of EVM (more than 10%) in order to provide time continuity between OFDM symbols. Since MSE criterion used in this article reflects the degradation due to time/frequency asynchronisms, EVM due to N-continuous OFDM generation is not taken into account.

In FMT case, we can observe that there is no (or negligible) asynchronous interference. Such a result is due to the fact that there is no (or negligible) interaction between subcarriers. Indeed, each FMT subcarrier can be seen as a traditional single carrier modulation which respects the Nyquist criteria thanks to the long transmit/receive FMT filters. Note that this excellent robustness against asynchronous interference is obtained to the detriment of latency which is very high in such a case (see Section IV-B).

Regarding FFT-FBMC case, one can observe that the MSE is almost between -30 dB and -38 dB except two regions:

- Inner subcarrier located at the edges of the useful RBs frequency bands, where the MSE is about -28 dB. Such a result can be explained by the fact the subcarrier gain at the RB edges is slightly lower than the gain of subcarriers located at the middle of the RB. In order to avoid this phenomenon and ensure a uniform gain for all RB subcarriers, a pre-distortion could be performed, as in BF-OFDM.
- Edge subcarriers (in the vicinity of interfering subcarriers), where the MSE varies from more than -10 dB when $\delta = 0$ Hz to -30 dB when $\delta = 75$ kHz. As in filter-bank WFs the edge subcarriers are highly impacted by interference but this distortion is spread over more than one subcarrier because of the non-uniform gain over RB subcarriers (i.e. the gain at the edge is weaker than the average gain).

Although the fact that BF-OFDM transmitter is similar to FFT-FBMC one, the performances are not the same. Indeed, BF-OFDM MSE is higher than FFT-FBMC one when the timing errors are outside the CP region. This is a direct consequence of the BF-OFDM receiver which is no more than the classical CP-OFDM receiver (i.e a simple FFT). In fact, the BF-OFDM rectangular receive filter brings an important amount of interference from the asynchronous user. However, the FFT-FBMC receiver is more efficient in asynchronous case thanks to the filtering performed by the analysis filter-bank. Note that, there is no asynchronous interference when the synchronization error does not exceed the CP (i.e. MSE about -65 dB corresponding to the intrinsic interference of the optimized BF-OFDM filter).

The average MSEs of WFs with complex orthogonality, obtained over all subcarriers, are plotted versus the TO for guard-bands $\delta = 0$ and 75 kHz, in Fig. 8.

In the CP region, we can observe that CP-OFDM and N-cont. OFDM achieve the best performance with a MSE lower than -60 dB. In UF-OFDM scheme, the ZP region is reduced to one sample period due to the fact that the ZP is fully employed to absorb the transmit filter transient response. In WOLA-OFDM, W-UF-OFDM and f-OFDM, the CP is no longer sufficient to deal with windowing or filtering effects giving rise to a slight distortion (between -40 to -35 dB) even in perfect synchronization case. The same remark can be made regarding FFT-FBMC and BF-OFDM, where the CP is used to absorb a part of the filtering effect.

When the delay errors exceed the CP interval, all schemes provide an improvement compared to CP-OFDM

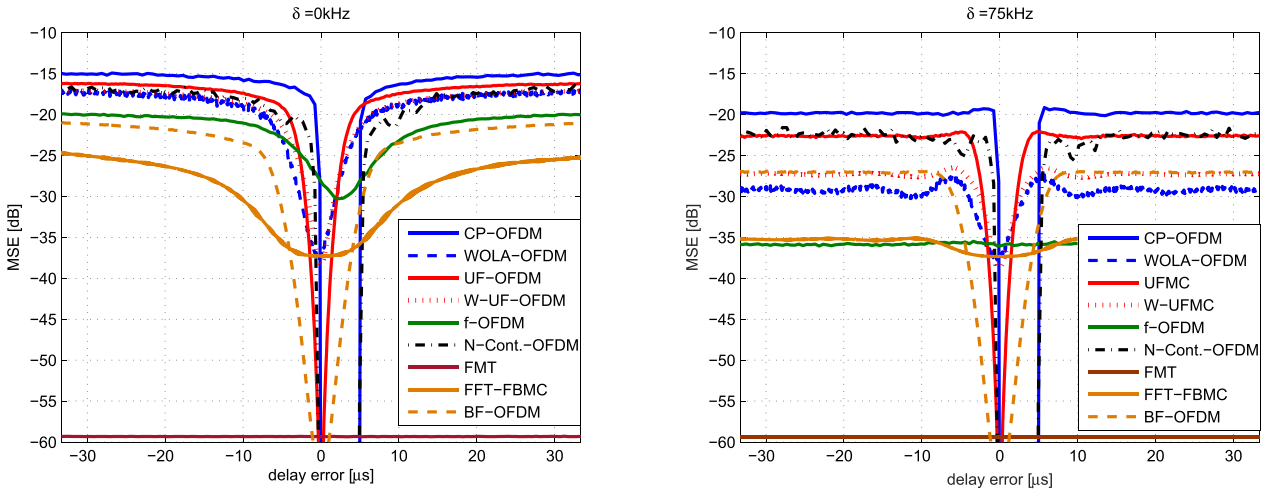

FIGURE 8. WFs with complex orthogonality: average MSE against TO, $\delta = 0$ and 75kHz (73.125kHz for FFT-FBMC and BF-OFDM).

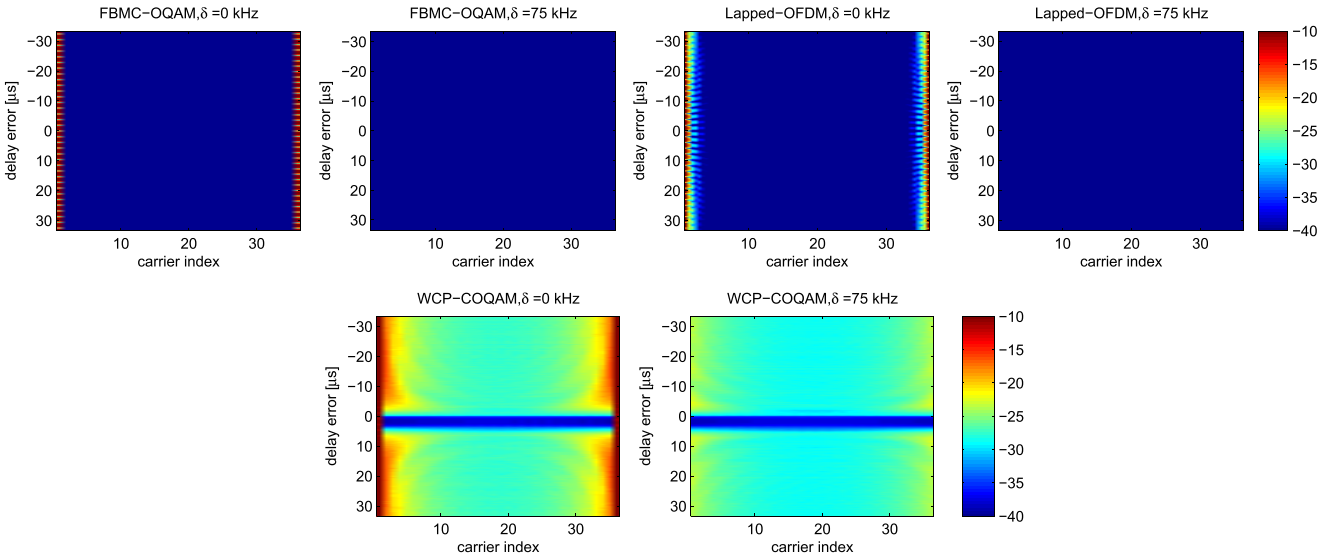

FIGURE 9. WFs with real orthogonality: per-subcarrier NMSE against TO, $\delta = 0$ and 75kHz.

performance which is severely degraded. In contrast to the marginal gain achieved by UF-OFDM and N-cont. OFDM systems, WOLA-OFDM, W-UF-OFDM and f-OFDM schemes are offering more significant enhancements reaching up to 7, 10 and 16 dB for W-UF-OFDM, WOLA-OFDM and f-OFDM, respectively (see $\delta = 75$kHz case). Moreover, we can see that FMT outperforms the rest of WFs by achieving the minimum MSE (about -60 dB) for the entire TO interval.

Looking at the average MSEs of FFT-FBMC and BF-OFDM, the results confirm the remarks previously noted when analyzing the per-subcarrier MSEs. Also, the best performance of FFT-FBMC is almost achieved when $\delta = 73.125$kHz while larger guard-bands can offer better performance in the BF-OFDM case. Such a result can be explained by the fact that the receive filtering of FFT-FBMC significantly reduces the asynchronous interference while the rectangular receive filter of BF-OFDM brings an important amount of interference from the coexisting asynchronous user. It is worth noticing that BF-OFDM performs better than FFT-FBMC in the CP-region since the prototype filter is designed to ensure the lowest degradation in negligible TO case.

b: WFs WITH REAL ORTHOGONALITY

The per-subcarrier MSEs of FBMC-OQAM (using PHYDYAS prototype filter), Lapped-OFDM and WCP-COQAM are respectively shown in Fig. 9. We can observe that a very small number of edge subcarriers are affected by interference thanks to the good spectral containment of FBMC-OQAM and Lapped-OFDM signals. Such a behavior is directly linked to the design of the prototype

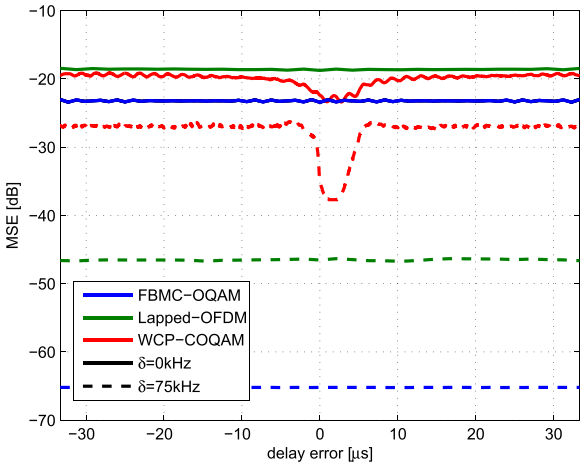

FIGURE 10. **WFs with real orthogonality: average MSE against TO, $\delta = 0$ and 75kHz.**

filter which is a key-property of FBMC WFs. Indeed, FBMC prototype filters are commonly designed in order to minimize the interaction between subcarriers (e.g. in PHYDYAS case, a subcarrier overlaps at most with a single subcarrier on each side). When increasing the guard-band size, FBMC can reach the FMT performance by offering a MSE below -40 dB for the entire useful frequency band.

In contrast to FBMC-OQAM and Lapped-OFDM, WCP-COQAM shows a completely different behavior. Let us recall that similarly to GFDM, a block based signal structure is adopted in WCP-COQAM thanks to the circular convolution property. In order to reduce the high-level spectrum side-lobes resulting from the inter-block discontinuities, a windowing is applied to the CP-COQAM signal. However, the windowing protection against asynchronous inter-user interference is less efficient compared to filtering one. This explains the poor WCP-COQAM performance in fully asynchronous case compared to FBMC-OQAM and Lapped-OFDM. However similar to CP based schemes, it should be pointed out that WCP-COQAM achieves a very low MSE inside the CP region when $\delta \geq 15$kHz.

The average MSEs of FBMC-OQAM, Lapped-OFDM and WCP-COQAM, computed over all subcarriers, are plotted w.r.t the TO for guard-bands $\delta = 0$ and 75 kHz, in Fig. 10. One can see that all OQAM-based schemes provide almost the same performance (MSE between 18dB for lapped-OFDM and 24 dB for FBMC-OQAM) when there is no guard-band between the useful frequency band and the interfering one. Note that the obtained average MSE is inversely related to the frequency bandwidth of the user of interest. However, the average MSE becomes independent of the latter when a sufficient guard-band is separating the interfering spectrum from the useful one. Indeed, the FBMC-OQAM MSE reaches its minimum value (about $-65dB$) and remains constant for $\delta \geq 15$kHz. The same result can be observed for Lapped-OFDM scheme but by inserting wider guard-bands. However, the WCP-COQAM still needs additional guard-band in order to reach its minimum MSE (about -38dB).

c: NON-ORTHOGONAL WFs

The per-subcarrier MSEs of FBMC-QAM and MF-GFDM are shown in Fig. 11 when the receiver is implemented without and with interference cancellation, respectively.

In the basic scheme (i.e. no interference cancellation), we can see that the MSE is almost the same for any subcarrier/TO for both FBMC-QAM and MF-GFDM. These strong MSE levels (dark orange color for MF-GFDM and red color for FBMC-QAM) are unfortunately meaningless to analyze the presence of asynchronous interference. In fact, since FBMC-QAM and MF-GFDM are non orthogonal, they suffer from a high level of self interference which makes us unable to distinguish the asynchronous interference from the self-distortion. In order to overcome this limitation, let us analyze the MSE when considering interference cancellation case: IC-FBMC-QAM and IC-MF-GFDM. The performances of IC-FBMC-QAM are almost similar to FBMC-OQAM where only a single subcarrier at each edge is impacted by the asynchronous interference. Such a result is due to the well-frequency localization of Samsung-Type-I prototype filter where a given subcarrier only interacts with its immediate adjacent subcarriers. Inserting a guard-band δ >15kHz (75kHz in this case) makes all useful subcarriers free from asynchronous interference. Regarding IC-MF-GFDM, one can see that asynchronous interference is more important on the edges of the useful frequency band. Thanks to transmit/receive filtering, the asynchronous interference decay becomes important when increasing the spectral distance between a given useful subcarrier and the interfering signal. Moreover, we can observe that the best performance is obtained when the TO is inside the CP interval except for the edge subcarriers when $\delta = 0$Hz.

Note that the interference cancellation based schemes severely increase the complexity of the receiver since the interference is estimated by the reconstruction of the a-priori transmitted signal.[4] It should be mentioned that the scenario considered is a noiseless case. These results are so a bound on the achievable performance. The interference cancellation scheme will suffer from noise and performance will be worst in case of AWGN channel.

The average MSEs of FBMC-QAM and MF-GFDM, computed over all subcarriers, are plotted w.r.t the TO for guard-bands $\delta = 0$ and 75 kHz, in Fig. 12. We can see that the FBMC-QAM MSE remains invariant with respect to the TO between the user of interest and the interfering one. For both guard-bands ($\delta = 0$ and 75kHz), the MSE is about -11dB due to the presence of high-level self-interference. After interference cancellation, we observe a significant improvement with -45dB of MSE when $\delta = 75$kHz. In contrast to the previous case, note that the MSE level when $\delta = 0$kHz is not conclusive since it is inversely proportional to the number of useful subcarrier. MF-GFDM has the same behaviour

[4]For simplicity sake, the interference cancellation [55] is limited to a single iteration

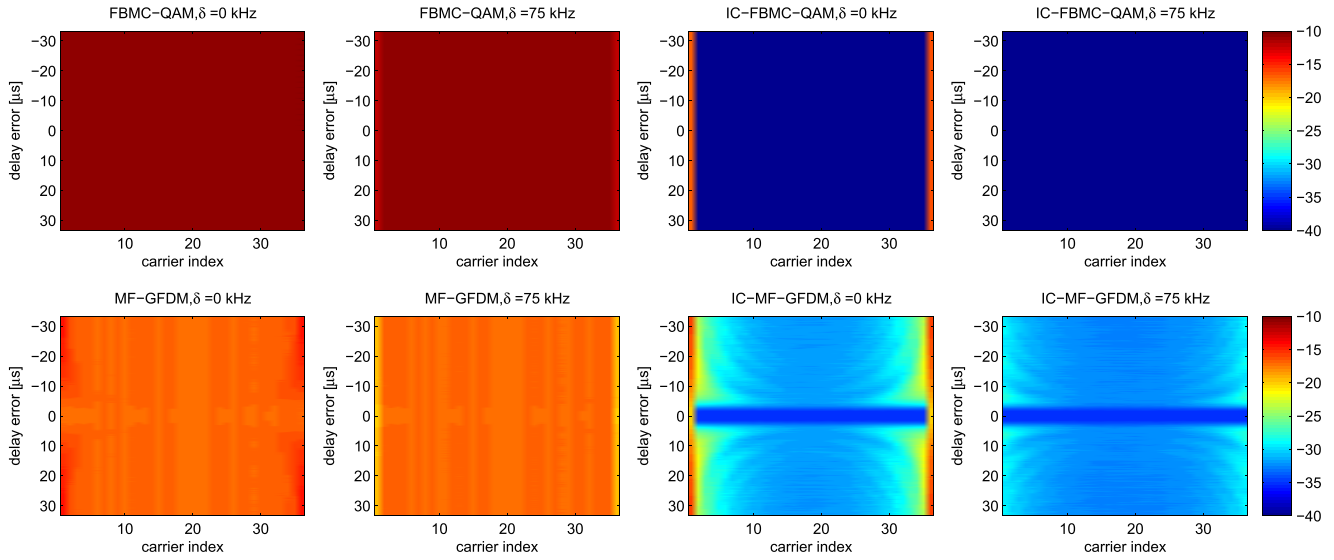

FIGURE 11. Non-orthogonal WFs without and with interference cancellation (IC): per-subcarrier NMSE against TO, $\delta = 0$ and 75kHz.

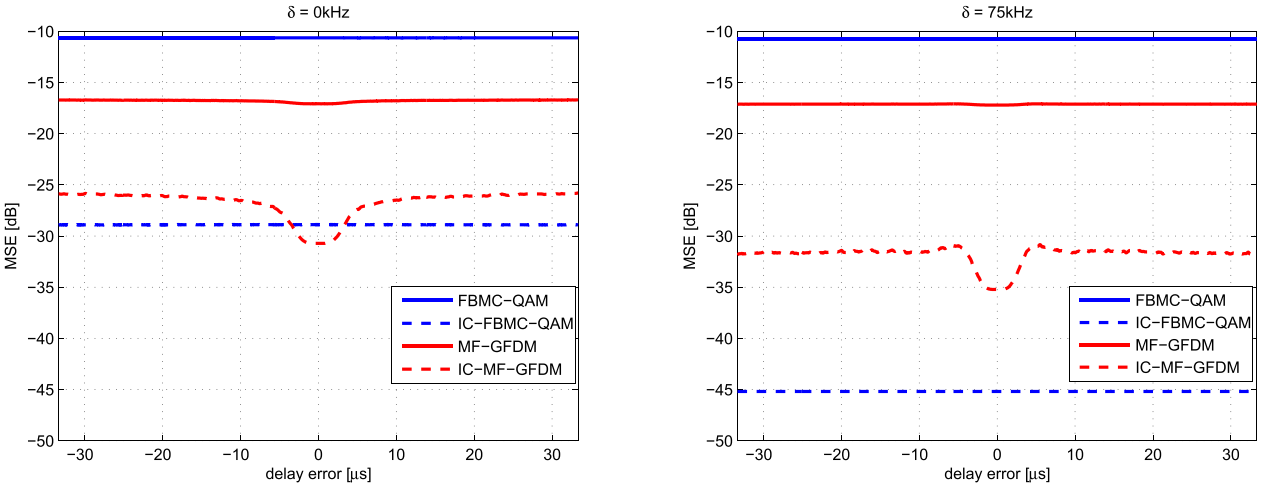

FIGURE 12. Non-orthogonal WFs: average MSE against TO, $\delta = 0$ and 75kHz.

but with an improvement weaker than the one provided by FBMC-QAM when $\delta = 75$kHz.

2) CARRIER FREQUENCY OFFSET

In this section, we assume that both users are perfectly synchronized in time domain but there is an offset between their respective carrier frequencies. The objective here is to examine the impact of CFO-induced inter-user interference on the performances of the various considered WFs. The CFO ε considered here varies from -1.5kHz to $+1.5$kHz. No guard-band is considered between the useful subcarriers and the interfering ones $\delta = 0$Hz. As mentioned in Section III, the CFO shifts both interfering spectrum subbands in the same direction. This is why one of the guard-bands is reduced to $\delta - \varepsilon$kHz and the other is increased to $\delta + \varepsilon$kHz.

a: WFs WITH COMPLEX ORTHOGONALITY

In Fig. 13, we have the per-subcarrier MSE of WFs with complex orthogonality.

In CP-OFDM and N-cont. OFDM cases, the edges subcarriers are more sensitive to CFO compared to inner ones. In fact, the MSE at the edges becomes important even for negligible CFO (from 150Hz) while inner subcarriers keep best performances (MSE< -30dB) even when $\varepsilon = 1.5$kHz.

In UF-OFDM case, the subcarriers located at the middle of useful frequency band are more protected, compared to CP-OFDM, against CFO where the MSE is below -40dB (dark-blue color).

When it comes to WOLA-OFDM, W-UF-OFDM and f-OFDM, the same behavior can be reported. Indeed, except the sensitivity of a few number of edge subcarriers to CFO when there is no guard-band, WOLA-OFDM and

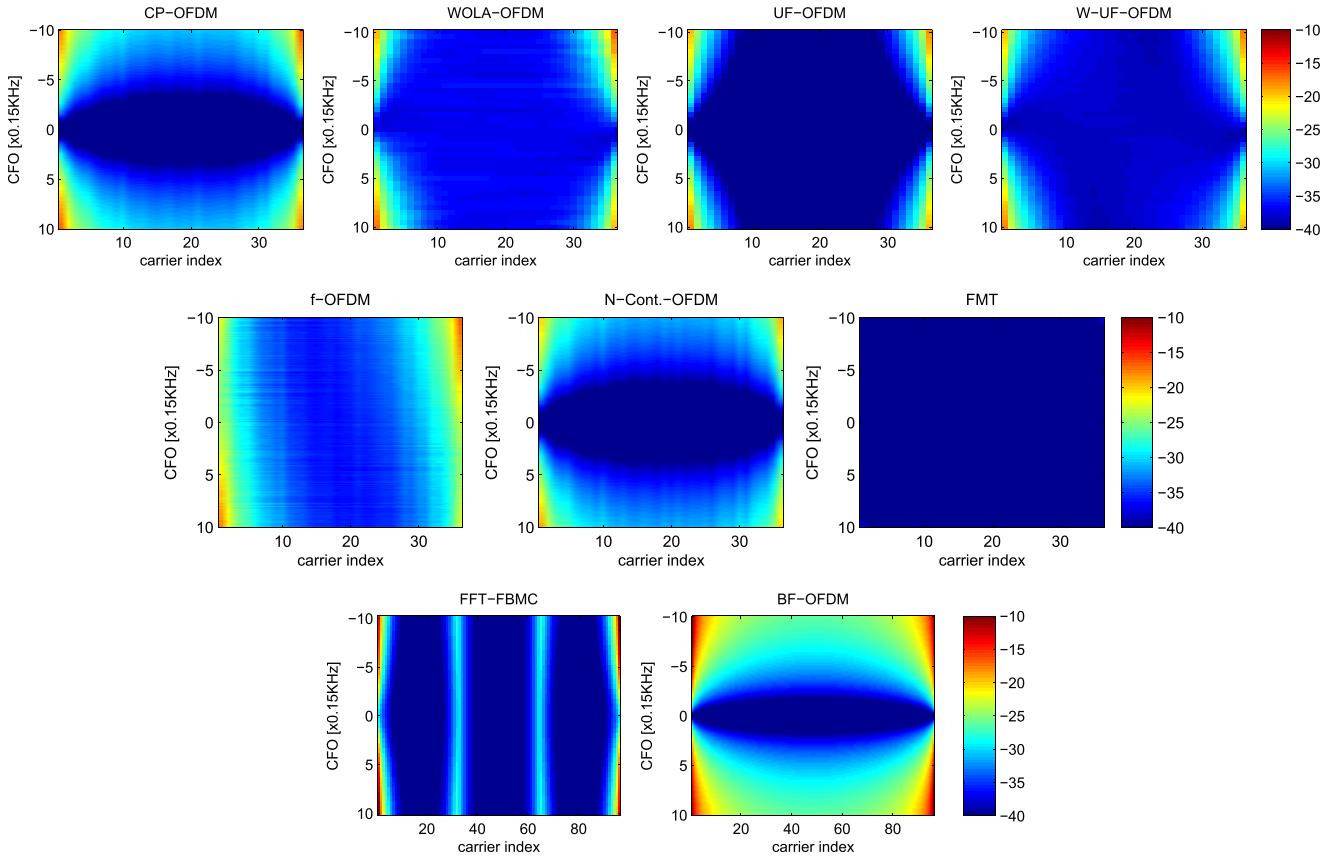

FIGURE 13. WFs with complex orthogonality: per-subcarrier NMSE against CFO, $\delta = 0$kHz.

W-UF-OFDM provide good performance with a MSE below −35dB for any subcarrier/CFO point. However, f-OFDM needs wider guard-band in order to ensure a uniform MSE for all useful subcarriers.

In FMT case, the best performance is achieved where a negligible MSE (dark-blue color : MSE less than −40dB) is shown for all useful subcarriers. This can be explained by the fact that the FMT prototype filter is extremely well frequency localized: the interferences are only produced by a single subcarrier at both edges of the useful bandwidth. For CFO values of about 10% or lower, the interferences created by this subcarrier is very small (lower than −40dB).

As in timing offset, FFT-FBMC exhibits almost the same MSE. Indeed, the MSE at the edges of each RB is about −30 dB, whereas it is less than −35 dB in the other subcarriers. As we have previously explained, this phenomenon is due to the filter shape in frequency domain. It is also worth noticing that except in both subcarrier edges the MSE is almost invariant with respect to CFO. In BF-OFDM case, the MSE is below −30 dB in a larger region around the CP one contrary to TO case where the MSE is very low only in the CP region.

The average MSEs of schemes with complex orthogonality, computed over all subcarriers, are plotted, in Fig. 14, as function of CFO. Looking at the different MSE curves, we

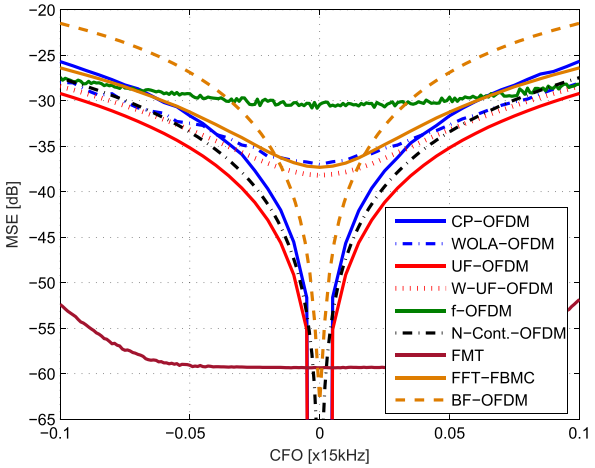

FIGURE 14. WFs with complex orthogonality: average MSE against CFO, $\delta = 0$kHz.

can distinguish three groups of WFs w.r.t to the sensitivity to CFO:

- weak sensitivity: in this group, we have f-OFDM and FMT. The MSE is practically invariant w.r.t to the considered CFO range.
- mild sensitivity: in WOLA-OFDM, W-UF-OFDM and FFT-FBMC cases, the variation of MSE is very slow when increasing CFO.

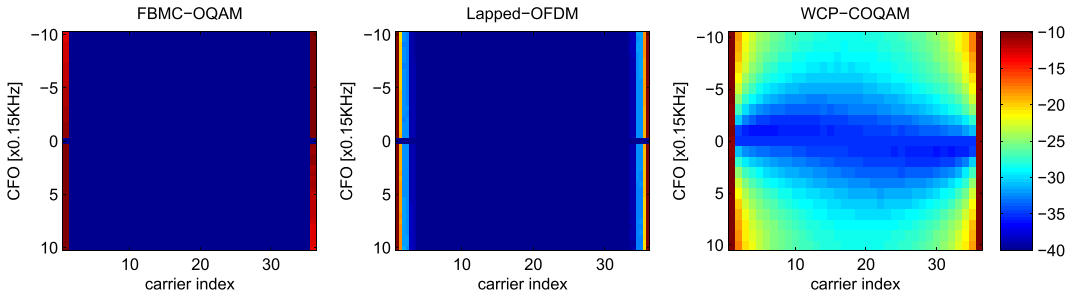

FIGURE 15. WFs with real orthogonality: per-subcarrier NMSE against CFO, $\delta = 0$kHz.

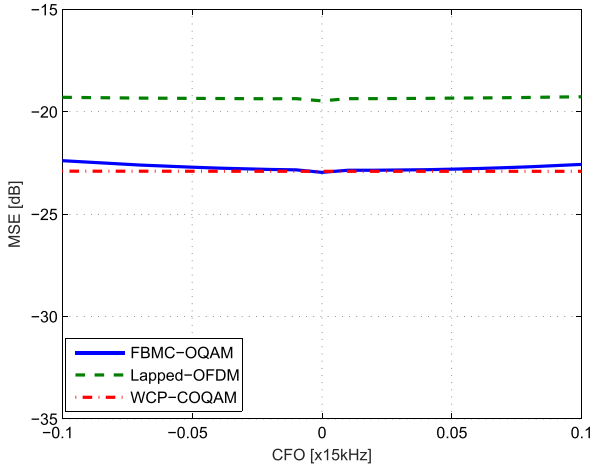

FIGURE 16. WFs with real orthogonality: average MSE against CFO, $\delta = 0$kHz.

- strong sensitivity: the MSEs of the other WFs is more important and rapidly grow with CFO.

b: WFs WITH REAL ORTHOGONALITY

The per-subcarrier CFO-induced MSEs of OQAM-based WFs are depicted in Figures 15. As previously discussed, the robustness against asynchronism is ensured thanks to transmit/receive filtering that limits the interaction between a given subcarrier and its neighborhood. Indeed, one can see that, similar to timing asynchronism, only a small number of subcarriers are suffering from asynchronous inter-user interference (e.g. one subcarrier on each side in FBMC-OQAM case).

Due to the block-based structure which is built-in property of WCP-COQAM signal, this scheme is more sensitive to CFO-induced inter-user interference compared to FBMC-OQAM and Lapped-OFDM systems. In fact, one can observe that the asynchronous interference caused by other user is more important, impacting thus a higher number of useful subcarriers compared to other OQAM-based WFs. Moreover, this interference is slowly decreasing w.r.t. to the spectral distance between a given victim subcarrier and the interfering signal.

The average MSE is plotted against the CFO for FBMC-OQAM, Lapped-OFDM and WCP-COQAM, in Fig. 16. In the absence of guard-bands between the useful spectrum and the interfering one, all OQAM-based WFs approximately show the same performance. It is worth pointing out that, the average MSE level does not really give a reliable information about the performances of the considered schemes, since it is inversely linked to the number of useful subcarriers.

c: NON-ORTHOGONAL WFs

The FBMC-QAM and MF-GFDM performances in terms of per-subcarrier MSE against CFO are depicted in Fig. 17.

Similar to the timing offset case, high level MSE (red color in FBMC-QAM and dark orange color in MF-GFDM) can be observed in the entire useful band for any CFO value, when there is no interference cancellation at the receiver side. Such a result is a natural outcome of the presence of the FBMC-QAM and MF-GFDM self interference. In order to better understand the asynchronous interference effect on the performance of both WFs, let us observe the MSE of these WFs with interference cancellation based-receivers. In IC-FBMC-QAM, since the considered CFO does not exceed the subcarrier spacing (i.e. $|\varepsilon_{max}| = 1.5$kHz), we can see that except the two subcarriers of the edges, the rest of useful subcarriers are completely protected against the asynchronous interference (it becomes almost negligible compared to the residual self-interference). In IC-MF-GFDM case, the asynchronous interference affects more than one subcarrier at each edge but the subcarriers located at the middle remain almost free of asynchronous interference.

Looking at the average MSEs of FBMC-QAM and MF-GFDM plotted against the CFO, we can see that MF-GFDM outperforms FBMC-QAM which means that the self-interference is higher in the latter. After interference cancellation, we can see that IC-FBMC-QAM becomes better than IC-MF-GFDM. Such a result is due to the fact that the asynchronous interference impact is more important in GFDM case. Similar to OQAM-based WFs, we recall that the average MSE remains not conclusive in this case, since it is inversely proportional to the number of useful subcarriers when there is no or insufficient guard-band between the useful and the interfering bands.

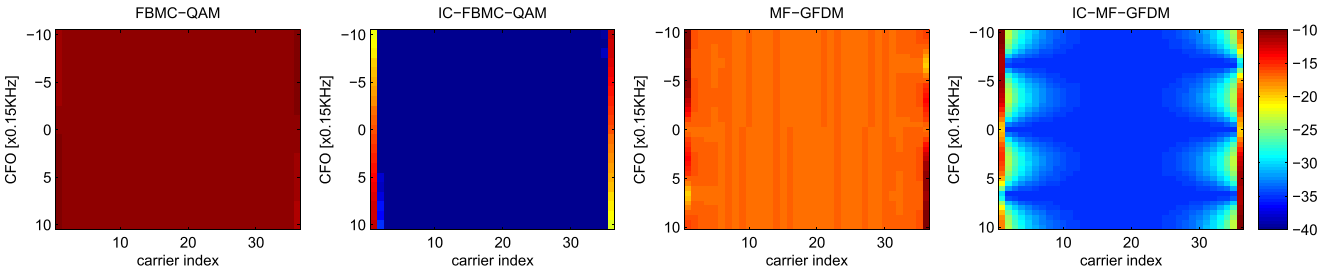

FIGURE 17. Non-orthogonal WFs: per-subcarrier NMSE against CFO, $\delta = 0$kHz.

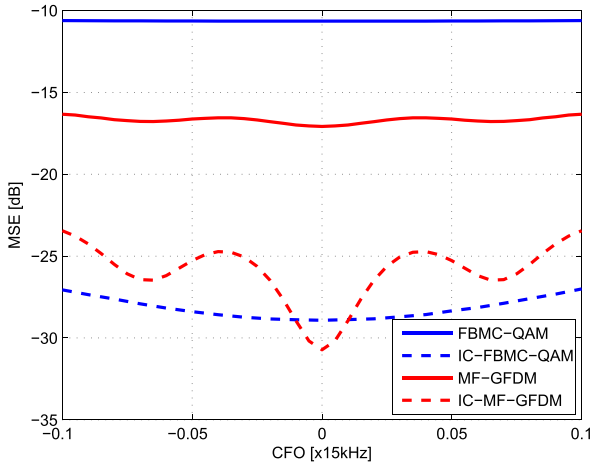

FIGURE 18. Non-orthogonal WFs: average MSE against CFO, $\delta = 0$kHz.

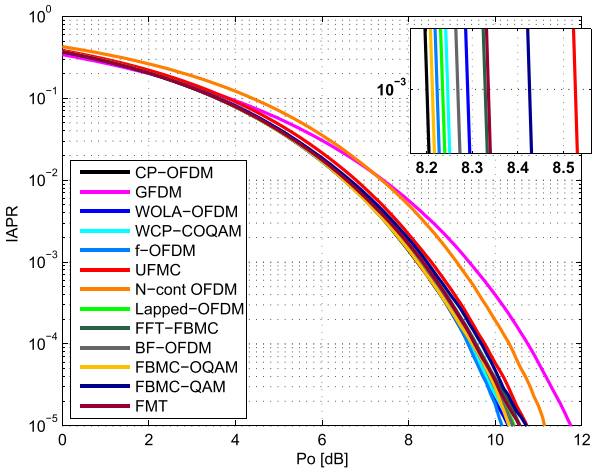

FIGURE 19. (Comparison of the CCDF of the IAPR.

D. IAPR

All multicarrier schemes have in common the major problem of very high fluctuation of the instantaneous power of the signal to be transmitted. More specifically, the probability of having an instantaneous power 8 to 12 dB greater than the mean power is non negligible. These instantaneous power peaks produce signal excursions into the nonlinear region of operation of the power amplifier (PA) at the RF front-end, generating distortions and spectral regrowth. Thus, it is important to assess and compare the performance in terms of power fluctuation of the considered WF. From a practical point of view, we believe that it is fairer and more relevant to consider the statistics of the samples that could go into the PA nonlinear area, instead of taking into account the sample with the highest power within a given period of time. For that reason, we consider in this paper the Instantaneous to Average Power Ratio (IAPR) criterion defined as the probability that the normalized instantaneous power exceeds a predefined threshold P_0 [57]:

$$IAPR\,[s(n)] = \text{Prob}\left[\frac{|s(n)|^2}{E\left[|s(n)|^2\right]} > P_0\right], \qquad (1)$$

where n refers to the time index of the whole signal to be transmitted.

From Fig. 19, we can observe that for a given number of active subcarriers, traditional CP-OFDM provides the best IAPR performance, which is in line with [58]. Nevertheless, all multicarrier WFs presented in this paper have almost equivalent IAPR performances, even if GFDM and N-continuous WFs have respectively 1 and 1.5 dB of degradation with respect to traditional CP-OFDM. It is important to note that there exist many techniques to reduce the IAPR which could be dedicated to a WF or generic, but the aim of these paper is not to address their respective performances.

E. COMPLEXITY

1) ANALYTICAL EXPRESSIONS

This section aims at estimating the complexity of the transmitter and receiver schemes for the considered WFs. The complexity will be assessed by counting the number of real multiplications per unit of time to perform both the modulation and demodulation process (equalization and (de)coding stages will not be taken into account in this evaluation). It has been preferred to assess the number of multiplications per unit of time in order to compare as fairly as possible the schemes that do not share the same sampling frequency. To do so, a burst of S symbol vectors (as defined in IV-B) is considered. For the schemes that exhibit symbol overlapping, the complexity will be benchmarked when S tends to infinity.

From now, it will be assumed that one complex multiplication can be carried out with three real multiplications [59]. F_s will denote the sampling frequency and T_s the sampling

period. Moreover, the Cooley-Tukey implementation will be considered for the Fast Fourier Transforms (FFT).

a: CP-OFDM

The complexity of the transmitter (resp. the receiver) is reduced to a N-points IFFT (resp. N-points IFFT), which leads to:

$$\mathrm{C}_{\mathrm{OFDM,Tx/Rx}} = \frac{3N_{\mathrm{FFT}}}{2}\log_2(N_{\mathrm{FFT}}) \tag{2}$$

The number of multiplications per unit of time is then:

$$\begin{aligned}\mathbb{C}_{\mathrm{OFDM,Tx/Rx}} &= \frac{\mathrm{C}_{\mathrm{OFDM,Tx/Rx}}S}{S(N_{\mathrm{FFT}}+N_{CP})T_s}\\ &= \frac{\mathrm{C}_{\mathrm{OFDM,Tx/Rx}}}{(N_{\mathrm{FFT}}+N_{CP})}F_s\end{aligned} \tag{3}$$

b: WOLA-OFDM

When it comes to WOLA-OFDM, the complexity also takes into consideration the windowing (real coefficients applied to complex data).

$$\mathrm{C}_{\mathrm{WOLA,Tx}} = \frac{3N_{\mathrm{FFT}}}{2}\log_2(N_{\mathrm{FFT}}) + 4\mathrm{W}_{\mathrm{Tx}} \tag{4}$$

$$\mathrm{C}_{\mathrm{WOLA,Rx}} = \frac{3N_{\mathrm{FFT}}}{2}\log_2(N_{\mathrm{FFT}}) + 4\mathrm{W}_{\mathrm{Rx}} \tag{5}$$

The number of multiplications per unit of time is then:

$$\begin{aligned}\mathbb{C}_{\mathrm{WOLA,Tx/Rx}} &= \frac{\mathrm{C}_{\mathrm{WOLA,Tx/Rx}}S}{(W_{\mathrm{Tx}}+S(N_{\mathrm{FFT}}+N_{CP}))T_s}\\ &\xrightarrow{S\to\infty} \frac{\mathrm{C}_{\mathrm{WOLA,Tx/Rx}}}{(N_{\mathrm{FFT}}+N_{CP})}F_s\end{aligned} \tag{6}$$

c: UF-OFDM

The data is processed at the RB level (B active RBs out of N_{FFT} available subcarriers). For each RB, first there is the predistortion stage with n complex multiplications. Then there is the transposition to the time domain with only n active sub carriers out of N_{FFT}. The IFFT is therefore mainly fed by null elements and its complexity can be reduced to $N_{\mathrm{FFT}} + \frac{N_{\mathrm{FFT}}}{2}\log_2(n)$ complex multiplications. The convolution with the baseband real filter (of length L_{FIR}) adds $N\lfloor\frac{L_{FIR}}{2}\rfloor$ multiplications (neglecting the rise and fall time of the convolution). Finally the upconversion to the carrier frequencies counts for $3(N_{\mathrm{FFT}}+L_{FIR}-1)$ real multiplications. At the receiver side, there is a $2N_{\mathrm{FFT}}$-point FFT. A windowing can be considered in reception which adds $2L_{R_x}$ multiplications and this receiver is denoted as wUF-OFDM .

$$\begin{aligned}\mathrm{C}_{\mathrm{UF-OFDM,Tx}} &= 3B\left(N_{\mathrm{FFT}} + \frac{N_{\mathrm{FFT}}}{2}\log_2(n)\right)\\ &\quad + 3B(N_{\mathrm{FFT}}+L_{FIR}-1) + 2BN_{\mathrm{FFT}}\lfloor\frac{L_{FIR}}{2}\rfloor\end{aligned} \tag{7}$$

$$\mathrm{C}_{\mathrm{UF-OFDM,Rx}} = 3N_{\mathrm{FFT}}\log_2(2N_{\mathrm{FFT}}) \tag{8}$$

$$\mathrm{C}_{\mathrm{wUF-OFDM,Rx}} = 3N_{\mathrm{FFT}}\log_2(2N_{\mathrm{FFT}}) + 2L_{R_x} \tag{9}$$

The number of multiplications per unit of time is then:

$$\begin{aligned}\mathbb{C}_{\mathrm{(w)UF-OFDM,Tx/Rx}} &= \frac{\mathrm{C}_{\mathrm{(w)UF-OFDM,Tx/Rx}}S}{S(N_{\mathrm{FFT}}+L-1)T_s}\\ &= \frac{\mathrm{C}_{\mathrm{UF-OFDM,Tx/Rx}}}{(N_{\mathrm{FFT}}+L-1)}F_s\end{aligned} \tag{10}$$

It must be pointed out that reduced complexity schemes have been proposed for UF-OFDM [60], [61] at the price of a slight performance degradation.

d: FILTERED OFDM

The complexity of this modulation scheme is induced by the (I)FFT and the filtering. The filter shape of length L is real and therefore the filtering operation is followed by a up-conversion addind $3\times(N_{\mathrm{FFT}}+N_{\mathrm{CP}}+L-1)$ extra real multiplications.

$$\begin{aligned}\mathrm{C}_{\mathrm{fOFDM,Tx/Rx}} &= \frac{3N_{\mathrm{FFT}}}{2}\log_2(N_{\mathrm{FFT}}) + 2\,(N_{\mathrm{FFT}}+N_{\mathrm{CP}})\lfloor\frac{L}{2}\rfloor\\ &\quad + 3(N_{\mathrm{FFT}}+N_{\mathrm{CP}}+L-1)\end{aligned} \tag{11}$$

The number of multiplications per unit of time is then:

$$\begin{aligned}\mathbb{C}_{\mathrm{fOFDM,Tx/Rx}} &= \frac{\mathrm{C}_{\mathrm{fOFDM,Tx/Rx}}S}{(L+S(N_{\mathrm{FFT}}+N_{CP}))T_s}\\ &\xrightarrow{S\to\infty} \frac{\mathrm{C}_{\mathrm{fOFDM,Tx/Rx}}}{(N_{\mathrm{FFT}}+N_{CP})}F_s\end{aligned} \tag{12}$$

e: N-CONTINUOUS OFDM

The complexity of the transmitter is induced by the FFT stage and the precoding (N_{FFT}^2 complex multiplications). The receiver is the same used in CP-OFDM.

$$\mathrm{C}_{\mathrm{NC-OFDM,Tx}} = 3N_{\mathrm{FFT}}^2 + \frac{3N_{\mathrm{FFT}}}{2}\log_2(N_{\mathrm{FFT}}) \tag{13}$$

$$\mathrm{C}_{\mathrm{NC-OFDM,Rx}} = \frac{3N_{\mathrm{FFT}}}{2}\log_2(N_{\mathrm{FFT}}) \tag{14}$$

The number of multiplications per unit of time is then:

$$\begin{aligned}\mathbb{C}_{\mathrm{NC-OFDM,Tx/Rx}} &= \frac{\mathrm{C}_{\mathrm{NC-OFDM,Tx/Rx}}S}{S(N_{\mathrm{FFT}}+N_{\mathrm{CP}})T_s}\\ &\xrightarrow{S\to\infty} \frac{\mathrm{C}_{\mathrm{NC-OFDM,Tx/Rx}}}{(N_{\mathrm{FFT}}+N_{CP})}F_s\end{aligned} \tag{15}$$

f: FMT

The FMT modulation is implemented by means of a polyphase network in both the transmitter and the receiver.

$$\mathrm{C}_{\mathrm{FMT,Tx/Rx}} = \frac{3N_{\mathrm{FFT}}}{2}\log_2(N_{\mathrm{FFT}}) + 2KN_{\mathrm{FFT}} \tag{16}$$

The number of multiplications per unit of time is then:

$$\begin{aligned}\mathbb{C}_{\mathrm{FMT,Tx/Rx}} &= \frac{\mathrm{C}_{\mathrm{FMT,Tx/Rx}}S}{(KN_{\mathrm{FFT}}+N_{\mathrm{FFT}}(S-1))T_s}\\ &\xrightarrow{S\to\infty} \frac{\mathrm{C}_{\mathrm{FMT,Tx/Rx}}}{N_{\mathrm{FFT}}}F_s\end{aligned} \tag{17}$$

g: FFT-FBMC

As for UF-OFDM, FFT-FBMC processes the data at the RB level. For each active RB (B out of M) there is the N-point IFFT and then there is the filter bank. The complexity of the receiver is the same.

$$\mathrm{C}_{\mathrm{FFT-FBMC,Tx/Rx}} = 3B\frac{N}{2}\left(1+\log_2\left(\frac{N}{2}\right)\right) + 2KMN + 3N\frac{M}{2}\log_2(M) \quad (18)$$

The number of multiplications per unit of time is then:

$$\mathbb{C}_{\mathrm{FFT-FBMC,Tx/Rx}} = \frac{\mathrm{C}_{\mathrm{FFT-FBMC,Tx/Rx}}S}{[KM+\frac{M}{2}(S(N+N_{CP})-1)]T_s} \xrightarrow{S\to\infty} \frac{\mathrm{C}_{\mathrm{FFT-FBMC,Tx/Rx}}}{\frac{M}{2}(N+N_{CP})}F_s \quad (19)$$

h: BF-OFDM

When it comes to BF-OFDM, at the transmitter side, there is an additional stage with respect to the FFT-FBMC scheme: the predistortion stage. Moreover, the receiver is reduced to a $\frac{MN}{2}$-point FFT.

$$\mathrm{C}_{\mathrm{BFOFDM,Tx}} = 3B\frac{N}{2} + 3B\frac{N}{2}\left(1+\log_2\left(\frac{N}{2}\right)\right) + 2KMN + 3N\frac{M}{2}\log_2(M) \quad (20)$$

$$\mathrm{C}_{\mathrm{BFOFDM,Rx}} = 3\frac{MN}{4}\log_2(\frac{MN}{2}) \quad (21)$$

The number of multiplications per unit of time is then:

$$\mathbb{C}_{\mathrm{BF-OFDM,Tx/Rx}} = \frac{\mathrm{C}_{\mathrm{BF-OFDM,Tx/Rx}}S}{[KM+\frac{M}{2}(S(N+N_{CP})-1)]T_s} \xrightarrow{S\to\infty} \frac{\mathrm{C}_{\mathrm{BF-OFDM,Tx/Rx}}}{\frac{M}{2}(N+N_{CP})}F_s \quad (22)$$

i: FBMC-OQAM AND LAPPED-OFDM

The complexity of FBMC/OQAM and Lapped-OFDM is related to the (I)FFT, the real filtering stage and the phase offset. The difference between the two modulation schemes is the considered overlapping factor (typically 4 for FBMC/OQAM and 2 for Lapped-OFDM). The complexities of the transmitter and receiver schemes are identical.

$$\mathrm{C}_{\mathrm{OQAM/Lapped,Tx/Rx}} = \frac{3N_{\mathrm{FFT}}}{2}\log_2(N_{\mathrm{FFT}}) + N_{\mathrm{FFT}}K + N_{\mathrm{FFT}} \quad (23)$$

The frequency-sampling scheme can also be considered [62]. It works with a KN_{FFT}-point (I)FFT and a pointwise filtering with $2K-1$ multiplications per symbol, and a phase offset.

$$\mathrm{C}_{\mathrm{FS,Tx/Rx}} = \frac{3KN_{\mathrm{FFT}}}{2}\log_2(KN_{\mathrm{FFT}}) + N_{\mathrm{FFT}}(2K-1) + N_{\mathrm{FFT}} \quad (24)$$

The number of multiplications per unit of time is then:

$$\mathbb{C}_{\mathrm{OQAM,Tx/Rx}} = \frac{\mathrm{C}_{\mathrm{OQAM,Tx/Rx}}S}{(KN_{\mathrm{FFT}}+\frac{N_{\mathrm{FFT}}}{2}(S-1))T_s} \xrightarrow{S\to\infty} \frac{\mathrm{C}_{\mathrm{OQAM,Tx/Rx}}}{\frac{N_{\mathrm{FFT}}}{2}}F_s \quad (25)$$

j: WCP-COQAM

At the transmitter side, $3\times\frac{N_{\mathrm{FFT}}}{2}\log_2(N_{\mathrm{FFT}})$ real multiplications are required for the IFFT and $3N_{\mathrm{FFT}}K^2$ real multiplications representing the additional arithmetic complexity [48]. Besides, $8W_{T_x}$ extra real multiplications are required for the windowing (real weighting shape).

For the receiver, KN_{FFT}-point FFT counts $3\frac{N_{\mathrm{FFT}}K}{2}\log_2(KN_{\mathrm{FFT}})$ real multiplications, the filtering requires $2N_{\mathrm{FFT}}(2K-1)$ real multiplications,[5] the K-point IFFT applied for each carrier requires $3N_{\mathrm{FFT}}K\log_2(2K)$ in total and the phase offset adds $2N_{\mathrm{FFT}}$ real multiplications.

$$\mathrm{C}_{\mathrm{WCP-COQAM,Tx}} = 3\frac{N_{\mathrm{FFT}}}{2}\log_2(N_{\mathrm{FFT}}) + 3N_{\mathrm{FFT}}K^2 + 8W_{\mathrm{T_x}} \quad (26)$$

$$\mathrm{C}_{\mathrm{WCP-COQAM,Rx}} = 3\frac{N_{\mathrm{FFT}}K}{2}\log_2(KN_{\mathrm{FFT}}) + 3N_{\mathrm{FFT}}K\log_2(2K) + 2N_{\mathrm{FFT}}(2K-1) \quad (27)$$

The number of multiplications per unit of time is then:

$$\mathbb{C}_{\mathrm{WCP-COQAM,Tx/Rx}} = \frac{\mathrm{C}_{\mathrm{WCP-COQAM,Tx/Rx}}2KS}{(KN_{\mathrm{FFT}}+N_{CP})ST_s} \xrightarrow{S\to\infty} \frac{2K\mathrm{C}_{\mathrm{WCP-COQAM,Tx/Rx}}}{KN_{\mathrm{FFT}}+N_{CP}}F_s \quad (28)$$

k: FBMC-QAM

The FBMC-QAM structure that is considered for this study is highly similar to the one used in FBMC-OQAM but with an Interference Cancellation stage at the receiver side. The IC block requires $3N_{\mathrm{FFT}}$ real multiplications induced by the MMSE detector. Another difference with respect to the FBMC-OQAM configuration is the use of a complex prototype filter. It is worth noticing that for this complexity study the MMSE coefficients are assumed to be know and their computation is not taken into account. In practice, the determination of those coefficients require matrix product et inversion operations and are therefore highly complex.

$$\mathrm{C}_{\mathrm{FBMC-QAM,Tx/Rx}} = \frac{3N_{\mathrm{FFT}}}{2}\log_2(N_{\mathrm{FFT}}) + 3N_{\mathrm{FFT}}K + 3N_{\mathrm{FFT}} \quad (29)$$

[5]Note that only a small portion of the filter frequency coefficients are non-zero-valued. Indeed, the number of non-zero coefficients of PHYDYAS filter is $2K-1$.

The number of multiplications per unit of time is then:

$$\mathbb{C}_{\text{FBMC-QAM,Tx/Rx}} = \frac{\text{C}_{\text{FBMC-QAM,Tx/Rx}} S}{(KN_{\text{FFT}} + N_{\text{FFT}}(S-1))T_s} \xrightarrow{S\to\infty} \frac{\text{C}_{\text{FBMC-QAM,Tx/Rx}}}{N_{\text{FFT}}} F_s \quad (30)$$

I: GFDM

The complexity of GFDM has been intensively studied in the literature and several articles have provided low complexity architectures for ZF/MF transmitter. Such architectures exploit the sparsity of the equivalent transmitter/receiver matrix to reduce the computational complexity without affecting the decoding performance. For the transmitter complexity evaluation, we use the framework described in [63]:

$$\text{C}_{\text{GFDM,Tx}} = \frac{3N_A \times N_B}{2} [3N_B + log_2(N_A)] \quad (31)$$

In this paper we consider a receiver based on match filtering and successive interference cancellation [55]. We use the receiver architecture proposed in [64] with I denotes the number of IC iterations:

$$\text{C}_{\text{GFDM,Rx}} = 3N_A \times N_B [log_2(N_A N_B) + log_2(N_B) + 6 + I(2log_2(N_A) + 1)] \quad (32)$$

The number of multiplications per unit of time is then:

$$\mathbb{C}_{\text{GFDM,Tx/Rx}} = \frac{\text{C}_{\text{GFDM,Tx/Rx}} S}{(N_A N_B + N_{CP}) ST_s} \xrightarrow{S\to\infty} \frac{\text{C}_{\text{GFDM,Tx/Rx}}}{N_A N_B + N_{CP}} F_s \quad (33)$$

2) ANALYSIS

According to the aforementioned closed-form expressions and the configurations given in III-B, it is possible to numerically assess the complexity of the different transmission and reception schemes as given in Tab. 7.

Due to its precoding stage, the N-Cont. OFDM is the most complex waveform with more than 205 times of the CP-OFDM complexity. Moreover, we can observe that waveforms relying on time convolution (UF-OFDM, f-OFDM) require a lot more computation resources for the transmitter scheme than the others. Note that, WCP-COQAM and GFDM are also more computation hungry.

On the contrary, waveforms based on polyphase network (FMT, FBMC-QAM, Lapped-OFDM and FBMC-QAM) provide an efficient hardware implementation. FFT-OFDM and BF-OFDM are more complex because of their precoding stage. As expected, the OFDM and the WOLA-OFDM are the least complex.

When it comes to the receiver schemes, waveforms relying on a simple FFT (OFDM, BF-OFDM, UF-OFDM, N-cont) with an eventual light receiver processing (WOLA-OFDM) perform well. UF-OFDM is slightly more complex because of its double size FFT while BF-OFDM is slightly more efficient thanks to its longer sampling period. Polyphase-network based receivers still perform well while the f-OFDM is still the more complex because of the time-convolution. WCP-COQAM and GFDM receivers are highly complex respectively because the oversampled-FFT and the interference cancellation stage.

TABLE 7. Tx/Rx complexity normalized with respect to OFDM.

WFs	Tx			Rx
	5RBs	25RBs	50RBs	
CP-OFDM	1.00	1.00	1.00	1.00
WOLA-OFDM	1.01	1.01	1.01	1.01
UF-OFDM	25.80	131.01	263.93	2.21
f-OFDM	37.85	37.85	37.85	37.85
N-Cont.-OFDM	205.80	205.80	205.80	1.00
FMT	3.35	3.35	3.35	3.35
FFT-FBMC	1.81	2.10	2.46	1.81
BF-OFDM	1.82	2.16	2.58	0.84
FBMC-OQAM	3.28	3.28	3.28	3.28
Lapped-OFDM	2.71	2.71	2.71	2.71
WCP-COQAM	3.29	3.29	3.29	17.41
FBMC-QAM	2.14	2.14	2.14	2.14
GFDM	3.28	3.28	3.28	9.03

V. EVALUATION AND DISCUSSIONS

In this section, our objective is to evaluate and discuss the simulation results obtained previously. It is not straightforward to rank the different criteria that have been analyzed in the light of MTC context. Nevertheless, from Section I, it has been highlighted that some criteria are of prime importance for this context such as: low latency, asynchronous capabilities, high reliability, high energy efficiency and spectral efficiency. Therefore, to give an overview on all of the considered WFs performance discussed previously, we introduce in Fig. 20 radar plots where each radar corresponds to one of the criteria summarized in Table 8. The corners here correspond to the considered WFs: CP-OFDM (WF01), WOLA-OFDM (WF02), UF-OFDM (WF03), f-OFDM (WF04), N-continuous OFDM (WF05), FMT (WF06), FFT-FBMC (WF07), BF-OFDM (WF08), FBMC-OQAM (WF09), Lapped-OFDM (WF10), WCP-COQAM (WF11), FBMC-QAM (WF12) and GFDM (WF13).

It should be noted that the PSD criterion can be related to the resistance to asynchronous users in the time domain. In fact, a WF with a very bad localized PSD will exhibit very bad performance concerning resistance to timing errors. Nevertheless, a WF with quite good spectral localization can have quite bad performance concerning resistance to timing errors if the receiving filter or windowing is not well localized in frequency. For instance, UF-OFDM and f-OFDM have a similar performance concerning their PSD but f-OFDM is better concerning TOs because of the receiving filter used in this WF. For these reasons, the PSD is not kept as a discriminant criterion even if it is very important that the transmitted signal respects a pre-defined spectral mask. This is also the case for the complexity.

Indeed, some WFs have a complexity lower than four times the complexity of CP-OFDM. For this set of WFs, complexity will not be a discriminant criterion. On the contrary a second

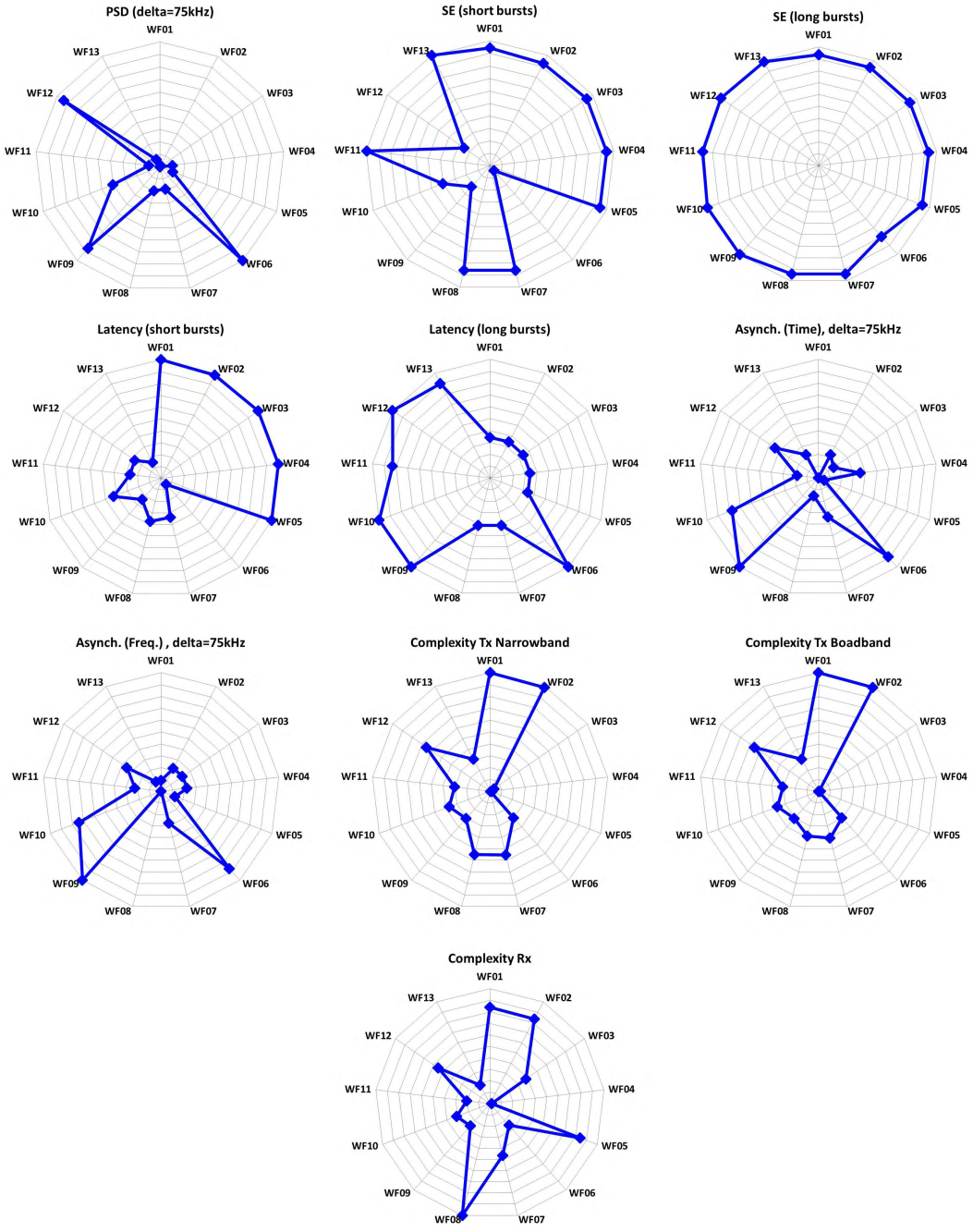

FIGURE 20. **Performance overview: CP-OFDM (WF01), WOLA-OFDM (WF02), UF-OFDM (WF03), f-OFDM (WF04), N-continuous OFDM (WF05), FMT (WF06), FFT-FBMC (WF07), BF-OFDM (WF08), FBMC-OQAM (WF09), Lapped-OFDM (WF10), WCP-COQAM (WF11), FBMC-QAM (WF12) and GFDM (WF13).**

set of WFs has a very high complexity (order of 100) compared to CP-OFDM: UF-OFDM, f-OFDM, N Cont.-OFDM and GFDM. For this second set of WFs, complexity can be a discriminant criterion.

In the following, a comparison based on discriminant criteria such as latency end-to-end (E2E) physical, latency, resistance to TO, resistance to CFO, Complexity, Spectral efficiency (SE) is hold between the previously mentioned WFs. Note that CP-OFDM is kept as a reference WF. Also, as the Lapped-OFDM and the FBMC-OQAM are very similar, only FBMC-OQAM is considered.

From Fig. 20, one can notice that some WFs with complex orthogonality such as WOLA-OFDM, UF-OFDM and f-OFDM have the CP-OFDM latency level, a more or less moderated added complexity and good performance concerning TOs and CFO.

TABLE 8. Comparison criteria specification.

Criterion	Specification
PSD	spectral distance of $\delta = 75$kHz
SE (short bursts)	a burst size = single multicarrier block
SE (long bursts)	a burst size = high number of multicarrier blocks
Latency (short bursts)	same as SE (short bursts)
Latency (long bursts)	same as SE (long bursts)
Robustness to TO	guard-band $\delta = 75$kHz
Robustness to CFO	guard-band $\delta = 75$kHz
Transmitter complexity (Narrow-Band case)	5RBs are used
Transmitter complexity (Broad-Band case)	50RBs are used
Receiver complexity	-

On the other hand, the N-continuous OFDM has worse TO and CFO performance and higher complexity than the CP-OFDM. Also, the FMT has higher latency and lower SE compared to the CP-OFDM. Moreover, for this WF there is a tradeoff between latency and SE. Note that, for better SE, a filter with a smaller roll-off factor is needed. This filter has a very long impulse response filter. Consequently, the latency is higher.

For WFs with real orthogonality and filtering applied to single subcarrier, the FBMC-OQAM, in comparison with OFDM, exhibits higher latency, better performance concerning TO and CFO and higher complexity. Nevertheless, the WCP-COQAM has poor performance concerning TO and CFO.

Finally, for WFs without orthogonality, the FBMC-QAM has higher latency, better TO and CFO performance and higher complexity than CP-OFDM. Differently, the GFDM has a very high complexity at the receiver side if interference cancellation is considered and poor performance in terms of TO and CFO.

VI. CONCLUSION

In this paper, we investigated the ability of post-OFDM WFs to support the C-MTC service which is one of the main technologies of the upcoming 5G. We provided a brief review highlighting the key design properties of each of these multicarrier WFs. After describing the common comparison framework, a global evaluation was performed while taking into account metrics such as PSD, spectral efficiency, End-to-End Physical layer latency, robustness to time and frequency synchronization errors, IAPR and transceiver computational complexity. Through this evaluation, we demonstrated that:

- Filtered WFs offered the best frequency localization especially when the spectral distance, separating the interfering and the useful signal, is small. However, the discussed filtered and windowed WFs granted satisfactorily low OOB compared to CP-OFDM when the spectral distance became larger.
- In short bursts case, all WFs gave almost the same spectral efficiency, except FBMC-OQAM, FMT and FBMC-QAM which are impacted by their respective long prototype filters. It is worth noticing that, despite their long filters, GFDM and WCP-COQAM provided better spectral efficiency thanks to the circular convolution. When it came to long bursts scenario, the filter impulse response length became negligible leading thus to the same spectral efficiency of the other WFs.
- When bursts are very short, OFDM-inspired WFs generated the lowest latencies compared to the other WFs that are affected by the ramp-up and the ramp down generated by the filtering operation. FMT yielded to the highest latency due its very long filter, making it unsuitable to C-MTC applications. In the case of very long bursts, WFs using CP or ZP gave higher latencies compared to the other WFs due to the number of CP/ZP added to the transmitted signal.
- Thanks to their well-frequency localized transmit/receive filters, FMT and FBMC-OQAM are the most robust against time and frequency synchronization errors. Also, FFT-FBMC, FBMC-QAM and f-OFDM provided good performances compared to CP-OFDM. The other WFs were more sensitive due to different reasons such as use of basic OFDM receiver for BF-OFDM, inefficiency of windowing when it is only applied on the edges of transmitted symbols/blocks.
- Regarding the transmitter' complexity, CP-OFDM and WOLA-OFDM granted the lowest level. In addition, N-cont. OFDM and UF-OFDM required huge computational resources reaching up to 200 times CP-OFDM complexity. The complexities of the other WFs remained tolerable with an order varying from less than twice to thirty times CP-OFDM complexity. It is worth recalling that UF-OFDM, FFT-FBMC and BF-OFDM Transmitter complexities was influenced by the number of active RBs.
- In contrast to the transmitter side, WOLA-OFDM, N-cont. OFDM and BF-OFDM receivers showed the best performance with a complexity similar to the CP-OFDM one. Except f-OFDM, WCP-COQAM and GFDM that are more computation-hungry, the other WFs require a reasonable computational cost.

Finally, the results shown in this study can be of great use to select the most suitable waveform to any C-MTC case according to its critical requirements.

REFERENCES

[1] 3GPP. (2015). *RAN 5G Workshop*. [Online]. Available: http://www.3gpp.org/newsevents/3gpp-news/1734-ran_5G
[2] *On Study on New Radio NR Access Technology: Physical Layer Aspects*, document RAN1 TR 38.802, Mar. 2017.

[3] D. Astely, E. Dahlman, G. Fodor, S. Parkvall, and J. Sachs, "LTE release 12 and beyond [accepted from open call]," *IEEE Commun. Mag.*, vol. 51, no. 7, pp. 154–160, Jul. 2013.

[4] "5G white paper," NGMN Alliance, Frankfurt, Germany, Feb. 2015. [Online]. Available: https://www.ngmn.org/fileadmin/ngmn/content/downloads/Technical/2015/NGMN_5G_White_Paper_V1_0.pdf

[5] G. Wunder *et al.*, "5GNOW: Non-orthogonal, asynchronous waveforms for future mobile applications," *IEEE Commun. Mag.*, vol. 52, no. 2, pp. 97–105, Feb. 2014.

[6] F. Zhao, "Smartphone solutions white paper," Shenzhen, China, Huawei, White Paper, Jul. 2012. [Online]. Available: http://www.huawei.com/ilink/en/download/HW_193034

[7] *R1-162199—Waveform Candidates*, Qualcomm, Incorp., San Diego, CA, USA, 2016.

[8] J. Abdoli, M. Jia, and J. Ma, "Filtered OFDM: A new waveform for future wireless systems," in *Proc. IEEE 16th Int. Workshop Signal Process. Adv. Wireless Commun. (SPAWC)*, Jun. 2015, pp. 66–70.

[9] J. van de Beek and F. Berggren, "N-continuous OFDM," *IEEE Commun. Lett.*, vol. 13, no. 1, pp. 1–3, Jan. 2009.

[10] M. Bellanger, "FBMC physical layer: A primer," ICT-PHYDYAS, Tech. Rep., Jun. 2010, pp. 1–31. [Online]. Available: http://www.ict-phydyas.org/teamspace/internal-folder/FBMC-Primer_06-2010.pdf

[11] M. Bellanger, D. Mattera, and M. Tanda, "Lapped-OFDM as an alternative to CP-OFDM for 5G asynchronous access and cognitive radio," in *Proc. IEEE Veh. Technol. Conf. (VTC Spring)*, May 2015, pp. 1–5.

[12] M. J. Abdoli, M. Jia, and J. Ma, "Weighted circularly convolved filtering in OFDM/OQAM," in *Proc. IEEE 24th Int. Symp. Pers. Indoor Mobile Radio Commun. (PIMRC)*, Sep. 2013, pp. 657–661.

[13] Y. H. Yun, C. Kim, K. Kim, Z. Ho, B. Lee, and J.-Y. Seol, "A new waveform enabling enhanced QAM-FBMC systems," in *Proc. IEEE 16th Int. Workshop Signal Process. Adv. Wireless Commun. (SPAWC)*, 2015, pp. 116–120.

[14] G. Cherubini, E. Eleftheriou, S. Oker, and J. M. Cioffi, "Filter bank modulation techniques for very high speed digital subscriber lines," *IEEE Commun. Mag.*, vol. 38, no. 5, pp. 98–104, May 2000.

[15] V. Vakilian, T. Wild, F. Schaich, S. ten Brink, and J.-F. Frigon, "Universal-filtered multi-carrier technique for wireless systems beyond LTE," in *Proc. IEEE Globecom Workshops (GC Wkshps)*, Dec. 2013, pp. 223–228.

[16] R. Gerzaguet *et al.*, "The 5G candidate waveform race: A comparison of complexity and performance," *EURASIP J. Wireless Commun. Netw.*, vol. 2017, no. 1, p. 13, 2017. [Online]. Available: http://dx.doi.org/10.1186/s13638-016-0792-0

[17] R. Zakaria and D. Le Ruyet, "A novel filter-bank multicarrier scheme to mitigate the intrinsic interference: Application to MIMO systems," *IEEE Trans. Wireless Commun.*, vol. 11, no. 3, pp. 1112–1123, Mar. 2012.

[18] G. Fettweis, M. Krondorf, and S. Bittner, "GFDM—Generalized frequency division multiplexing," in *Proc. IEEE 69th Veh. Technol. Conf. (VTC)*, Apr. 2009, pp. 1–4.

[19] P. Banelli, S. Buzzi, G. Colavolpe, A. Modenini, F. Rusek, and A. Ugolini, "Modulation formats and waveforms for 5G networks: Who will be the heir of OFDM?: An overview of alternative modulation schemes for improved spectral efficiency," *IEEE Signal Process. Mag.*, vol. 31, no. 6, pp. 80–93, Nov. 2014.

[20] A. Sahin, I. Guvenc, and H. Arslan, "A survey on multicarrier communications: Prototype filters, lattice structures, and implementation aspects," *IEEE Commun. Surveys Tuts.*, vol. 16, no. 3, pp. 1312–1338, 3rd Quart., 2014.

[21] B. Farhang-Boroujeny, "OFDM versus filter bank multicarrier," *IEEE Signal Process. Mag.*, vol. 28, no. 3, pp. 92–112, May 2011.

[22] R. Gerzaguet, J.-B. Dore, N. Cassiau, and D. Kténas, "Comparative study of 5G waveform candidates for below 6 GHz air interface," in *Proc. ETSI Workshop Future Radio Technol. Focusing Air Interface*, 2016, pp. 1–16.

[23] C. Ibars, U. Kumar, H. Niu, H. Jung, and S. Pawar, "A comparison of waveform candidates for 5G millimeter wave systems," in *Proc. 49th Asilomar Conf. Signals, Syst. Comput.*, Nov. 2015, pp. 1747–1751.

[24] B. Farhang-Boroujeny and H. Moradi, "OFDM Inspired Waveforms for 5G," *IEEE Commun. Surveys Tuts.*, vol. 18, no. 4, pp. 2474–2492, 4th Quart., 2016.

[25] M. Van Eeckhaute, A. Bourdoux, P. De Doncker, and F. Horlin, "Performance of emerging multi-carrier waveforms for 5G asynchronous communications," *EURASIP J. Wireless Commun. Netw.*, vol. 2017, no. 1, p. 29, 2017. [Online]. Available: http://dx.doi.org/10.1186/s13638-017-0812-8

[26] Q. Bodinier, F. Bader, and J. Palicot, "On spectral coexistence of CP-OFDM and FB-MC waveforms in 5G networks," *IEEE Access*, vol. 5, pp. 13883–13900, 2017.

[27] Y. Medjahdi, M. Terré, D. L. Ruyet, D. Roviras, and A. Dziri, "Performance analysis in the downlink of asynchronous OFDM/FBMC based multi-cellular networks," *IEEE Trans. Wireless Commun.*, vol. 10, no. 8, pp. 2630–2639, Aug. 2011.

[28] Q. Bodinier, F. Bader, and J. Palicot, "Coexistence in 5G: Analysis of cross-interference between OFDM/OQAM and legacy users," in *Proc. IEEE Globecom Workshops (GC Wkshps)*, Dec. 2016, pp. 1–6.

[29] X. Zhang, L. Chen, J. Qiu, and J. Abdoli, "On the waveform for 5G," *IEEE Commun. Mag.*, vol. 54, no. 11, pp. 74–80, Nov. 2016.

[30] A. A. Zaidi *et al.*, "A preliminary study on waveform candidates for 5G mobile radio communications above 6 GHz," in *Proc. IEEE 83rd Veh. Technol. Conf. (VTC Spring)*, May 2016, pp. 1–6.

[31] B. Saltzberg, "Performance of an efficient parallel data transmission system," *IEEE Trans. Commun. Technol.*, vol. COM-15, no. 6, pp. 805–811, Dec. 1967.

[32] R. Zayani, Y. Medjahdi, H. Shaiek, and D. Roviras, "WOLA-OFDM: A potential candidate for asynchronous 5G," in *Proc. IEEE Global Commun. Conf. (GLOBECOM)*, Dec. 2016, pp. 1–5.

[33] Y. Medjahdi, R. Zayani, H. Shaïek, and D. Roviras, "WOLA processing: A useful tool for windowed waveforms," in *Proc. IEEE Int. Conf. Commun. (ICC)*, May 2017, pp. 393–398.

[34] T. Wild, F. Schaich, and Y. Chen, "5G air interface design based on universal filtered (UF-)OFDM," in *Proc. IEEE Int. Conf. Digit. Signal Process. (DSP)*, Aug. 2014, pp. 699–704.

[35] B. Muquet, Z. Wang, G. B. Giannakis, M. D. Courville, and P. Duhamel, "Cyclic prefixing or zero padding for wireless multicarrier transmissions?" *IEEE Trans. Commun.*, vol. 50, no. 12, pp. 2136–2148, Dec. 2002.

[36] F. Schaich and T. Wild, "Relaxed synchronization support of universal filtered multi-carrier including autonomous timing advance," in *Proc. 11th Int. Symp. Wireless Commun. Syst. (ISWCS)*, Aug. 2014, pp. 203–208.

[37] "f-OFDM scheme and filter design," Huawei HiSilicon, 3GPP, Nanjing, China, document R1-165425, TSG RAN WG1 Meeting #85, May 2016. [Online]. Available: http://portal.3gpp.org/ngppapp/CreateTdoc.aspx?mode=view&contributionId=708027

[38] J. van de Beek and F. Berggren, "EVM-constrained OFDM precoding for reduction of out-of-band emission," in *Proc. IEEE 70th Veh. Technol. Conf. Fall*, Sep. 2009, pp. 1–5.

[39] S. Traverso, "A family of square-root Nyquist filter with low group delay and high stopband attenuation," *IEEE Commun. Lett.*, vol. 20, no. 6, pp. 1136–1139, Jun. 2016.

[40] F. J. Harris, C. Dick, and M. Rice, "Digital receivers and transmitters using polyphase filter banks for wireless communications," *IEEE Trans. Microw. Theory Techn.*, vol. 51, no. 4, pp. 1395–1412, Apr. 2003.

[41] R. Zakaria and D. Le Ruyet, "A novel FBMC scheme for spatial multiplexing with maximum likelihood detection," in *Proc. 7th Int. Symp. Wireless Commun. Syst. (ISWCS)*, Sep. 2010, pp. 461–465.

[42] R. Zakaria and D. Le Ruyet, "Theoretical analysis of the power spectral density for FFT-FBMC signals," *IEEE Commun. Lett.*, vol. 20, no. 9, pp. 1748–1751, Sep. 2016.

[43] R. Zakaria and D. Le Ruyet, "FFT-FBMC equalization in selective channels," *IEEE Signal Process. Lett.*, vol. 24, no. 6, pp. 897–901, Jun. 2017.

[44] D. Demmer, R. Gerzaguet, J.-B. Doré, D. Le Ruyet, and D. Kténas, "Block-filtered OFDM: An exhaustive waveform to overcome the stakes of future wireless technologies," in *Proc. IEEE Int. Conf. Commun. (ICC)*, Paris, France, May 2017, pp. 1–6.

[45] A. Viholainen, T. Ihalainen, T. H. Stitz, M. Renfors, and M. Bellanger, "Prototype filter design for filter bank based multicarrier transmission," in *Proc. 17th Eur. Signal Process. Conf.*, Aug. 2009, pp. 1359–1363.

[46] F. Schaich, T. Wild, and Y. Chen, "Waveform contenders for 5G—Suitability for short packet and low latency transmissions," in *Proc. IEEE 79th Veh. Technol. Conf. (VTC Spring)*, May 2014, pp. 1–5.

[47] M. Bellanger, "Efficiency of filter bank multicarrier techniques in burst radio transmission," in *Proc. IEEE Global Telecommun. Conf. (GLOBECOM)*, Dec. 2010, pp. 1–4.

[48] H. Lin and P. Siohan, "Multi-carrier modulation analysis and WCP-COQAM proposal," *EURASIP J. Adv. Signal Process.*, vol. 2014, no. 1, 2014, Art. no. 79. [Online]. Available: https://doi.org/10.1186/1687-6180-2014-7

[49] C. Lélé, P. Siohan, and R. Legouable, "The Alamouti Scheme with CDMA-OFDM/OQAM," *EURASIP J. Adv. Signal Process.*, vol. 2010, no. 1, 2010, Art. no. 703513. [Online]. Available: http://dx.doi.org/10.1155/2010/703513
[50] R. Zakaria and D. Le Ruyet, "Intrinsic interference reduction in a filter bank-based multicarrier using QAM modulation," *Phys. Commun.*, vol. 11, pp. 15–24, Jun. 2014.
[51] R. Zakaria, D. Le Ruyet, and Y. Medjahdi, "On ISI cancellation in MIMO-ML detection using FBMC/QAM modulation," in *Proc. IEEE Int. Symp. Wireless Commun. Syst. (ISWCS)*, Aug. 2012, pp. 949–953.
[52] O. E. Agazzi and N. Seshadri, "On the use of tentative decisions to cancel intersymbol interference and nonlinear distortion (with application to magnetic recording channels)," *IEEE Trans. Inf. Theory*, vol. 43, no. 2, pp. 394–408, Mar. 1997.
[53] S. Van Beneden, J. Riani, and J. W. Bergmans, "Cancellation of linear intersymbol interference for two-dimensional storage systems," in *Proc. IEEE Int. Conf. Commun.*, vol. 7. Jun. 2006, pp. 3173–3178.
[54] N. Michailow, I. Gaspar, S. Krone, M. Lentmaier, and G. Fettweis, "Generalized frequency division multiplexing: Analysis of an alternative multi-carrier technique for next generation cellular systems," in *Proc. Int. Symp. Wireless Commun. Syst. (ISWCS)*, Aug. 2012, pp. 171–175.
[55] R. Datta, N. Michailow, M. Lentmaier, and G. Fettweis, "GFDM interference cancellation for flexible cognitive radio PHY design," in *Proc. IEEE Veh. Technol. Conf. (VTC Fall)*, Sep. 2012, pp. 1–5.
[56] N. Michailow, S. Krone, M. Lentmaier, and G. Fettweis, "Bit error rate performance of generalized frequency division multiplexing," in *Proc. IEEE Veh. Technol. Conf. (VTC Fall)*, Sep. 2012, pp. 1–5.
[57] C. Ciochina, F. Buda, and H. Sari, "An analysis of OFDM peak power reduction techniques for WiMAX systems," in *Proc. IEEE Int. Conf. Commun. (ICC)*, vol. 10. Jun. 2006, pp. 4676–4681.
[58] M. Chafii, J. Palicot, R. Gribonval, and F. Bader, "A necessary condition for waveforms with better PAPR than OFDM," *IEEE Trans. Commun.*, vol. 64, no. 8, pp. 3395–3405, Aug. 2016.
[59] S. G. Krantz, *Handbook of Complex Variables*. Basel, Switzerland: Birkhäuser, 1999.
[60] M. Matthe, D. Zhang, F. Schaich, T. Wild, R. Ahmed, and G. Fettweis, "A reduced complexity time-domain transmitter for UF-OFDM," in *Proc. IEEE 83rd Veh. Technol. Conf. (VTC Spring)*, May 2016, pp. 1–5.
[61] T. Wild and F. Schaich, "A reduced complexity transmitter for UF-OFDM," in *Proc. IEEE 81st Veh. Technol. Conf. (VTC Spring)*, May 2015, pp. 1–6.
[62] M. Bellanger, "FS-FBMC: A flexible robust scheme for efficient multicarrier broadband wireless access," in *Proc. IEEE Globecom Workshops (GC Wkshps)*, Dec. 2012, pp. 192–196.
[63] A. Farhang, N. Marchetti, and L. E. Doyle, "Low-complexity modem design for GFDM," *IEEE Trans. Signal Process.*, vol. 64, no. 6, pp. 1507–1518, Mar. 2016.
[64] I. Gaspar, N. Michailow, A. Navarro, E. Ohlmer, S. Krone, and G. Fettweis, "Low complexity GFDM receiver based on sparse frequency domain processing," in *Proc. IEEE 77th Veh. Technol. Conf. (VTC Spring)*, Jun. 2013, pp. 1–6.

YAHIA MEDJAHDI received the degree in engineering from the École Nationale Polytchnique of Algiers, Algeria, the M.Sc. degree in signal processing for communications from the Institute Galilée, Paris 13 University, in 2008, and the Ph.D. degree from the Conservatoire National des Arts et Métiers (CNAM), in 2012. He was a Researcher with the CEDRIC Laboratory, CNAM, an Assistant Professor with Khemis-Miliana University, Algeria, and a Post-Doctoral Researcher with the ICTEAM Laboratory, Université Catholique de Louvain, Belgium. He is currently an Assistant Professor with the Institut Supérieur d'Électronique de Paris. He has been involved in several ICT-European and French projects, such as PHYDYAS, EMPHATIC, and WONG5, dealing with waveform design for 5G and PMR systems. He has authored or co-authored 30 papers in peer-reviewed journals and international conferences, and one book chapter. His research interests include flexible multicarrier waveform design, cooperative communications, PAPR reduction, and non-linearity of power amplifiers.

SYLVAIN TRAVERSO received the M.Sc. degree from the École Nationale Supérieure de l'Électronique et de ses Applications in 2002 and the Ph.D. degree from Cergy Pontoise University, France, in 2007. In 2008, he joined Thales Communications and Security, as a Signal Processing Specialist, where he is currently in charge of developing the physical layers of HF/VUHF military radios, and also in charge of digital compensation algorithms of radio frequency impairments, such as IQ imbalance and power amplifier non-linearity. He has authored papers in international conferences and journals, and four patents. His current research interests are in the area of multicarrier schemes, new wireless access technologies, and radio architectures.

ROBIN GERZAGUET received the degree in electrical engineering from the Grenoble Institute of Technology, France, in 2011, and the Ph.D. degree from the Gipsa-Laboratory, University of Grenoble and ST-Microelectronics, in 2015. He is currently with CEA-Leti, where he was involved in physical layer and filter bank multicarrier waveforms in the context of millimeter wave transmissions. His research interests are in signal processing algorithms dedicated to communication, including channel estimation, synchronization, and digital RF impairments compensation.

HMAIED SHAÏEK received the Engineer degree from the National Engineering School of Tunis in 2002, and the master's degree from the Université de Bretagne Occidentale in 2003, and the Ph.D. degree from the Lab-STICC CNRS Team, Telecom Bretagne, in 2007. He was with Canon Inc., until 2009. He left the industry to integrate with the École Nationale d'Ingénieurs de Brest as a Lecturer, from 2009 to 2010. In 2011, he joined the CNAM, as an Associate Professor in electronics and signal processing. He has authored or co-authored three patents, six journal papers, and over 25 conference papers. His research activities focus on performances analysis of multicarrier modulations with nonlinear power amplifiers, PAPR reduction, and power amplifier linearization. He contributed to the FP7 EMPHATIC European project and is involved in two national projects, such as Accent5 and Wong5, funded by the French National Research Agency. He has co-supervised three Ph.D. students and four master students.

RAFIK ZAYANI received the Engineer, M.Sc. and Ph.D. degrees from the École Nationale d'Ingénieurs de Tunis (ENIT) in 2003, 2004, and 2009, respectively. He was with the Laboratory of Communications Systems (Sys'Com), ENIT, from 2003 to 2005. Since 2005, he has been with the Innov'COM laboratory, Sup'Com School, Tunisia. From 2004 to 2009, he was with the Department of Telecommunication and Networking, Institut Supérieur d'Informatique (ISI), Tunis, as a contractual Assistant Professor. Since 2009, he has been an Associate Professor (tenure position) with the ISI, Tunisia. Since 2010, he has been an Associate Researcher with the CEDRIC Laboratory, Conservatoire National des Arts et Métiers, France. He is an Established Researcher with long experience in multicarrier communications, energy efficiency enhancement by: transmitter linearization techniques (baseband DPD) and PAPR reduction; high power amplifier characterization; neural network; identification modeling and equalization; and MIMO technologies. He was involved in enhanced multicarrier waveforms, such as FBMC-OQAM, UFMC, GFDM, BFOFDM, and WOLA-OFDM. He has contributed in several European (EMPHATIC) and French (WONG5) projects that aim at designing flexible air-interfaces for future wireless communications (5G and Beyond).

DAVID DEMMER received the engineering degree in electronics from the Grenoble Institute of Technology, France, in 2015. He is currently pursuing the Ph.D. degree with the Conservatoire National des Arts et Métiers and CEA-Leti. His current research interest lies in filter bank-based waveforms and multiple-antenna systems.

ROSTOM ZAKARIA received the engineering degree in electronics from the University of Science and Technology Houari Boumediene, Algiers, Algeria, in 2007, and the M.Sc. degree from the University of Paris-Est de Marne-La-Vallée, France, in 2008, and the Ph.D. degree from the CEDRIC/LAETITIA Research Laboratory, Conservatoire National des Arts et Métiers (CNAM), Paris, in 2012. Since 2012, he has been a temporary Assistant Professor and a Researcher with CNAM. His research interests are interference cancellation techniques in the filter bank-based multicarrier modulations, spatial time and frequency coding in FBMC, and device-to-device communications.

JEAN-BAPTISTE DORÉ received the M.S. degree from the Institut National des Sciences Appliquées (INSA), Rennes, France, in 2004, and the Ph.D. degree in joint code design and decoding architecture for LDPC codes from the France Telecom Research and Development, Orange Labs, and INSA, Rennes, France, in 2007. He was a Signal Processing Architect with NXP semiconductors, home business unit Caen, France. He was in charge on the study and design of signal processing algorithms for DVB-T/DVB-T2 products (OFDM waveforms). In 2009, he joined as a Research Engineer with the Centre for Atomic Energy, CEA-Minatec, Grenoble, France. He has authored or co-authored around 50 papers in international conference proceedings and book chapters, has also been involved in standardization group (IEEE1900.7) and is the main inventor of over 20 patents. His main research topics are signal processing such as multicarriers, OFDM, FBMC, and single carrier, hardware architecture optimizations, and PHY and MAC layers for wireless network. He was involved in many projects including UWB, RFID, and Cellular network technologies, as an Architect for PHY and MAC layer (studies and implementation). He is currently involved in the definition of 5G system (PHY). He was a recipient of the ICC 2017 Best Paper Award.

MOUNA BEN MABROUK received the degree in electronic and telecommunication engineering from the University of Carthage, Tunisia, in 2012, the Ph.D. degree from the IMS laboratory, University of Bordeaux, about power amplifier behavior modeling in a CR context to develop an energy efficient digital linearization technique and as a Student with the University of Bordeaux, France, in 2015. She is currently holds a post-doctoral position with the IETR Laboratory, CentraleSupelec, where she is involved in post-OFDM waveforms for 5G systems.

DIDIER LE RUYET (SM'11) received the Eng. and Ph.D. degrees from the Conservatoire National des Arts et Métiers (CNAM), Paris, in 1994 and 2001, respectively, and the Habilitation à diriger des recherches degree from Paris XIII University in 2009. From 1988 to 1996, he was a Senior Member of the Technical Staff with SAGEM Defense and Telecommunication, France. He joined as a Research Assistant with the Signal and Systems Laboratory, CNAM, in 1996. From 2002 to 2010, he was an Assistant Professor with the Electronic and Communication Laboratory, CNAM. Since 2010, he has been a Full Professor with the CEDRIC Research Laboratory, CNAM. He has authored or co-authored over 100 papers in refereed journals and conference proceedings and six books/book chapters in the area of communication. He has been involved in several National and European projects dealing with multicarrier transmission techniques and multi-antenna transmission. His main research interests lie in the areas of digital communications and signal processing, including channel coding, detection, and estimation algorithms, filter bank-based multi-carrier communication, and multi-antenna transmission. He served as a Technical Program Committee member in major the IEEE conferences such as ICC, GLOBECOM, VTC, ISWCS, and WCNC. He was the General Chair for ISWCS 2012 and a Co-General Chair for ISWCS 2014. He served as a Co-Editor of a special issue of *EURASIP Journal on Wireless Communications and Networking* on recent advances in multiuser MIMO systems.

YVES LOUËT received the Ph.D. degree in digital communications from Rennes University, France, in 2000, and the HDR degree from Rennes University in 2010. His Ph.D. thesis was on peak to average power reduction in OFDM modulation with channel coding. He was a Research Engineer with SIRADEL Company, Rennes, France, in 2000, where he was involved in channel propagation modeling for cell planning. He was with French collaborative research projects, including COMMINDOR, ERASME, and ERMITAGES about channel modeling in many frequency bands, especially, 60 and 5 GHz for further telecommunication systems. In 2002, he was an Associate Professor with Supelec, Rennes. He became a Professor with Supelec. He is currently with CentraleSupelec. He is the Co-Head of the Signal Communication Embedded Electronics Research Group, a member of the Institute of Electronics and Telecommunications of Rennes Laboratory, and the Vice-Chair of the URSI Commission C. His teaching and research activities have been in regard signal processing and digital communications applied to software and cognitive radio systems. He was involved in many collaborative European projects, including FP7E2R, CELTIC B21C, CELTIC SHARING, NoE Newcom, and COST and French projects, including ANR PROFIL, ANR INFOP, FUI AMBRUN, TEPN, and WINOCOD. His research contribution is mainly focused on new waveforms design for green cognitive radio and energy efficiency enhancement.

DANIEL ROVIRAS was born in 1958. He received the Engineer degree from SUPELEC, Paris, France, in 1981, and the Ph.D. degree from the National Polytechnic Institute of Toulouse, Toulouse, France, in 1989. He spent in the industry as a Research Engineer for seven years. He joined the Electronics Laboratory, École Nationale Supérieure d'Électrotechnique, d'Électronique, d'Informatique, et des Télécommunications (ENSEEIHT). In 1992, he joined the Engineering School, ENSEEIHT, as an Assistant Professor, where he has been a Full Professor since 1999. Since 2008, he has been a Professor with the Conservatoire National des Arts et Métiers (CNAM), Paris, France, where his teaching activities are related to radio-communication systems. He is currently a member of the CEDRIC Laboratory, CNAM. His research activity was first centered around transmission systems based on infrared links. Since 1992, his topics have widened to more general communication systems, such as mobile and satellite communications systems, equalization, and predistortion of nonlinear amplifiers, and multicarrier systems.